ACI STRUCTURAL JOURNAL TECHNICAL PAPER

Title no. 92-S9

Code Background Paper:*

Concrete Capacity Design (CCD) Approach for Fastening to Concrete



by Werner Fuchs, Rolf Eligehausen, and John E. Breen

A user-friendly, highly transparent model for the design of post-installed steel anchors or cast-in-place headed studs or bolts, termed the concrete capacity design (CCD) approach, is presented. This approach is compared to the well-known provisions of ACI 349-85. The use of both methods to predict the concrete failure load of fastenings in uncracked concrete under monotonic loading for important applications is compared. Variables included single anchors away from and close to the edge, anchor groups, tension loading, and shear loading. A data bank including approximately 1200 European and American tests was evaluated. The comparison shows that the CCD method can accurately predict the concrete failure load of fastenings for the full range of investigated applications. On the other hand, depending on the application in question, the predictions of ACI 349 are sometimes unconservative and sometimes conservative. The CCD method is more user-friendly for design. Based on this, the CCD method is recommended as the basis for the design of fastenings.

Keywords: anchors (fasteners); **concretes**; failure; **fasteners**; loads (forces); shear tests; **structural design**; studs; tension tests.

The demand for more flexibility in the planning, design, and strengthening of concrete structures has resulted in an increased use of metallic anchoring systems. Currently employed are cast-in situ anchors such as headed studs [Fig. 1(a)] or headed bolts and fastening systems to be installed in hardened concrete, such as torque-controlled expansion anchors [Fig. 1(b)], deformation-controlled expansion anchors [Fig. 1(c)], undercut anchors [Fig. 1(d)], and adhesive anchors [Fig. 1(e)].

Cast-in situ elements are fastened to the formwork and cast into the concrete. A common example is a plate with welded-on headed studs [Fig. 1(a)], which produces mechanical interlocking with the concrete.

Post-installed anchors can be fastened in almost any position desired in hardened concrete by installing them in a hole drilled after concrete curing. A distinction is drawn between metal expansion anchors, undercut anchors, and bonded anchors, according to their principles of operation.

Expansion anchors produce expansion forces and thereby (frictional) holding forces in the concrete base material. With torque-controlled expansion anchors [Fig. 1(b)], a specified installation torque is applied. Thereby, one cone or two cones, according to the type of anchor, is/are drawn into the expanding sleeve or segments. Torque-controlled anchors should expand further under load. Deformation-controlled anchors [(Fig. 1(c)] are expanded by driving the cone into the sleeve [drop-in anchor, Fig. $1(c_1)$] or onto the cone [Fig. $1(c_2)$ (self-drilling anchor) and Fig. $1(c_3)$ (steel anchor)] through a specified displacement. Deformation-controlled anchors cannot expand further under load.

Undercut anchors are anchors with parts that spread and mechanically interlock with the concrete base material. After production of the cylindrical hole by drilling, the undercutting is produced in a second operation before installation of the anchor [Fig. $1(d_1)$ through $1(d_3)$] or during installation of the anchor [Fig. $1(d_4)$ and $1(d_5)$]. Much lower expansion forces are produced during installation and loading than with expansion anchors. In fact, certain undercut anchors can act virtually identically to cast-in anchors if the angle and diameter at the undercut are within certain limits.

The operating principle of adhesive anchors [Fig. 1(e)] depends on gluing together a threaded rod and the wall of the drilled hole with reacting resins. The load is transferred to the concrete base material by chemical bonding. Adhesive anchors are not covered in this paper.

BEHAVIOR UNDER TENSION LOADING

Under tension loading, fastening systems can experience four different types of failures (Fig. 2), each with very different load-deformation patterns, as shown in Fig. 3. Fig. 3 is valid for anchors with relatively low remaining prestressing

*ACI Committee 318 has endorsed early publication of this paper which serves as background to upcoming code revisions.

ACI Structural Journal, V. 92, No. 1, January-February 1995.

Received Feb. 2, 1994, and reviewed under Institute publication policies. Pertinent discussion will be published in the November-December 1995 *ACI Structural Journal* if received by July 1, 1995.

Werner Fuchs *is Manager, Innovation of the Hilti Development Corp., Kaufering, Germany. He received his diploma degree in civil engineering from the University of Karlsruhe and PhD from the University of Stuttgart, Germany. After a postdoctoral fellowship at the University of Texas at Austin, he joined Hilti. He has conducted research and written extensively on topics related to techniques for fastening to concrete. He is a member of ACI 355, Anchorage to Concrete.*

ACI member ***Rolf Eligehausen*** *is a Professor and Department Head for fastening technique at the Institute for Building Materials, University of Stuttgart. He studied at the University of Braunschweig and obtained his PhD from the University of Stuttgart in 1979. After 2 years of research work at the University of California at Berkeley, he returned to the University of Stuttgart and was appointed to the rank of Professor in 1984. He is a member of several international committees on reinforced concrete and fastening technique, and has published several papers in these fields. He is a member of ACI Committee 355, Anchorage to Concrete.*

ACI honorary member ***John E. Breen*** *holds the Nasser I. Al-Rashid Chair in Civil Engineering at the University of Texas at Austin. He began research work in fastening to concrete in 1963. He is a member and former chairman of ACI 318, Building Code, and is former chairman of the ACI Technical Activities Committee. He is an associate member of ACI Committee 355, Anchorage to Concrete.*

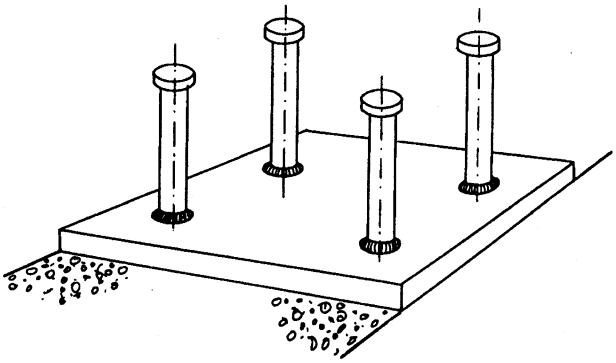

Fig. 1(a) —Fastening systems: headed studs

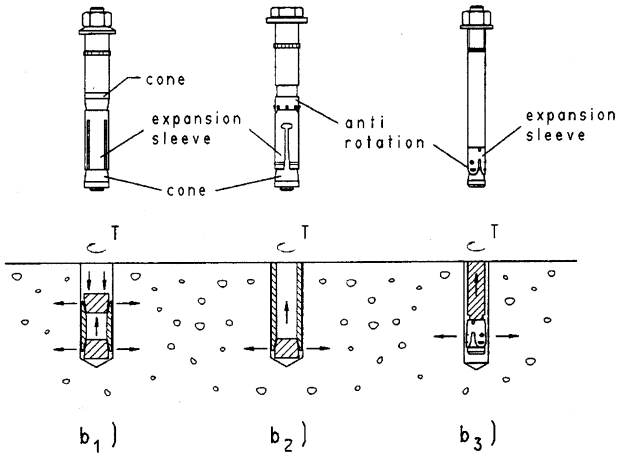

Fig. 1(b) —Fastening systems: torque-controlled expansion anchor (upper sketches show assembled anchors; lower sketches show anchor mechanism actions)

force after losses due to relaxation and other similar effects. The magnitude of the prestressing force will influence the behavior of the anchor at service load levels but has practically no influence at failure load levels.

Pullout or *pullthrough* failures are failure by sliding out of the fastening device or parts of it from the concrete (pullout) or by pulling the cone through the sleeve (pullthrough) without the breaking out of a fairly substantial portion of the surrounding concrete [Fig. 2(c)]. For deformation-controlled fasteners, only the pullout failure mode is possible.

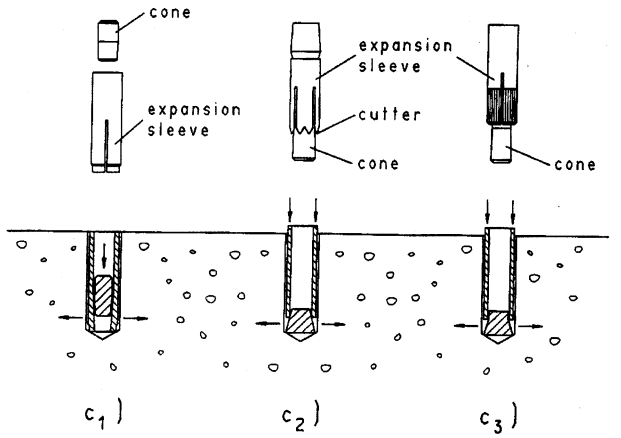

Fig. 1(c) — Fastening systems: deformation-controlled expansion anchor (upper sketches show assembled anchors; lower sketches show anchor mechanism actions)

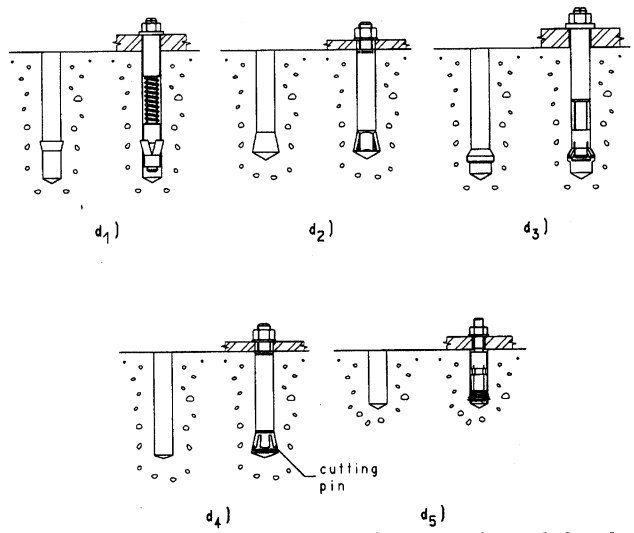

Fig. 1(d) —Fastening systems: undercut anchors (left-side sketches show hole shape; right-side sketches show installed anchors)

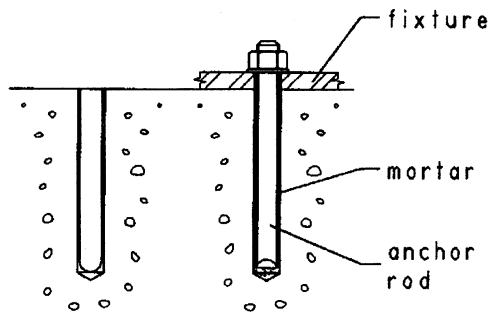

Fig. 1(e) —Fastening systems: bonded or adhesive anchors (left-side sketches show hole shape; right-side sketches show installed anchors)

For expansion anchors, the failure load depends on the design of the expansion mechanism, method of drilling the hole, condition of the drilled hole, and deformability of the concrete. Currently, there is no established procedure to determine theoretically the ultimate load to be expected of fastenings in the pullout or pullthrough type of failure. It must be determined in comprehensive prequalification tests, such

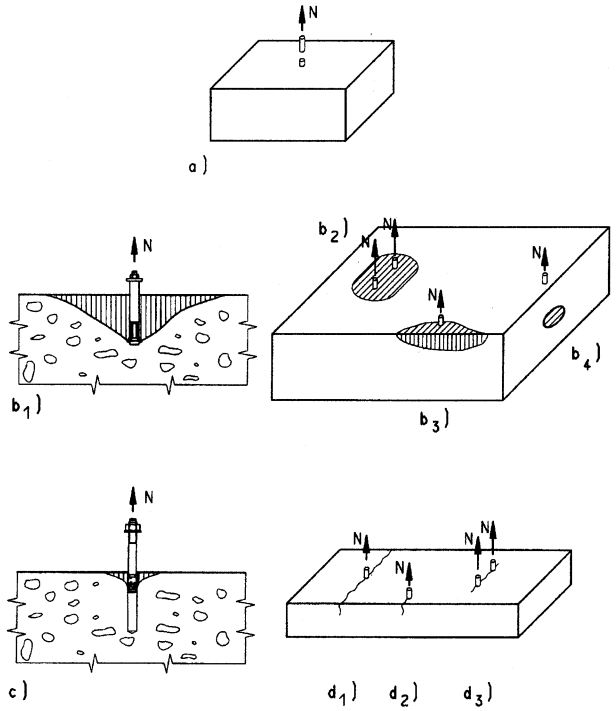

Fig. 2—Failure modes for fastenings under tensile loading: (a) steel failure; (b) concrete breakout; (c) pullout; (d) concrete splitting

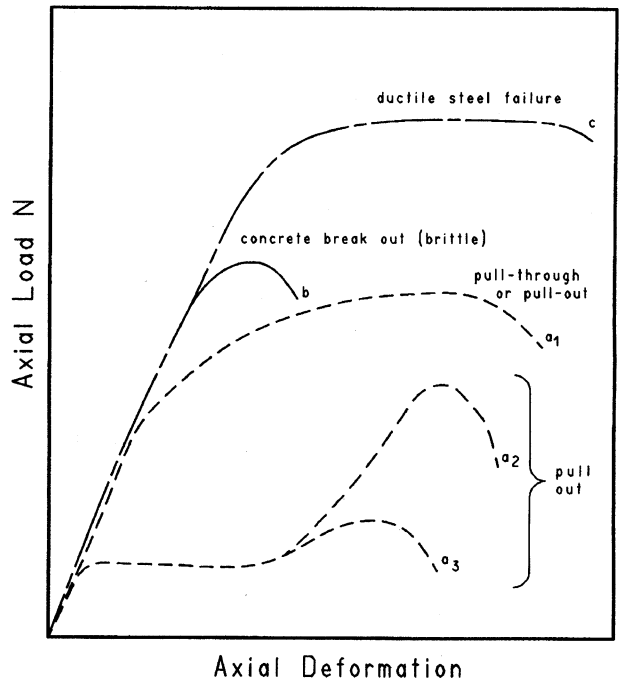

Fig. 3—Idealized load-deformation curves for fasteners under tension load

as those proposed in ASTM ZXXX.[1] In the case of a pull-through failure, in general the load-displacement relationship continuously increases and failure occurs at relatively large displacements (Line a_1 in Fig. 3). This anchor behavior is mainly dependent on the quality of the anchor production, and is acceptable in many applications.

In contrast, in the case of a pullout failure, the load-displacement curve may increase continuously until peak load (Line a_1 in Fig. 3) or the anchor may slip significantly in the hole at a load level larger than the remaining prestressing force of the anchor (Lines a_2 and a_3 in Fig. 3) before expanding further and developing a higher load capacity. This behavior is influenced considerably by the installation procedure and is highly undesirable. It must be prohibited by performance requirements in prequalification testing of the fastening device.

With expansion anchors, the depth of embedment can control the type of failure. As shown in Fig. 4, there is a critical embedment depth later termed h_{ef}, the effective embedment depth, at which the mode of failure changes from concrete failure to pullout. This depends on the expansion mechanism and h_{ef} is determined in prequalification tests.

The concrete bearing area of undercut anchors and headed studs is usually large enough to prevent pullout failure.

Ductile failures are failure by yielding of the fastening device or system fastened to the concrete before any breakout of concrete occurs [Fig. 2(a)].

Under conditions that the steel material is sufficiently ductile and the length of the fastener or attachment over which inelastic steel strains appear is large enough, and assuming that the concrete base material does not fail, a ductile steel failure will occur (Line c in Fig. 3).

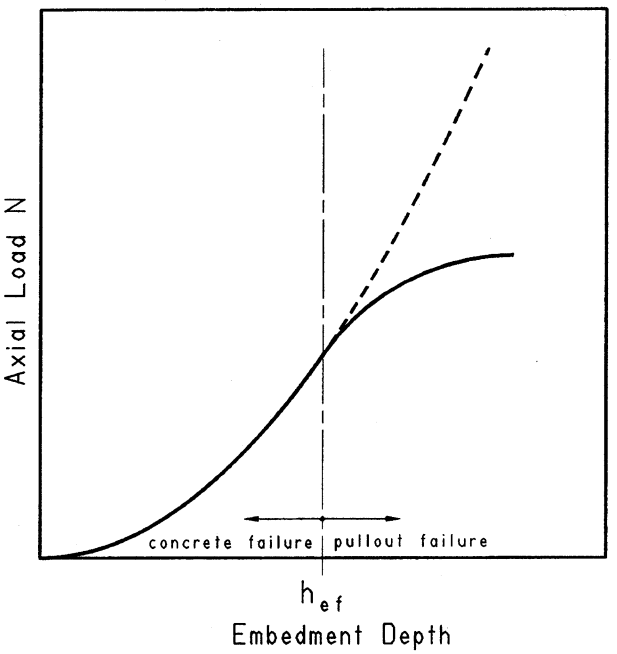

Fig. 4—Role of effective depth h_{ef} *for expansion anchors*

Brittle failures are failure by concrete breakout or splitting of the structural concrete member before yielding of the fastener or fastened element [Fig. 2(b) and (d)] or by steel failure when the length over which inelastic steel strains appear is rather small.

For nonductile fasteners and cases where the concrete capacity is less than the fastener device capacity, a brittle failure will occur (Line b in Fig. 3).

It is not yet possible to determine theoretically the failure load to be expected in the "splitting" type of failure

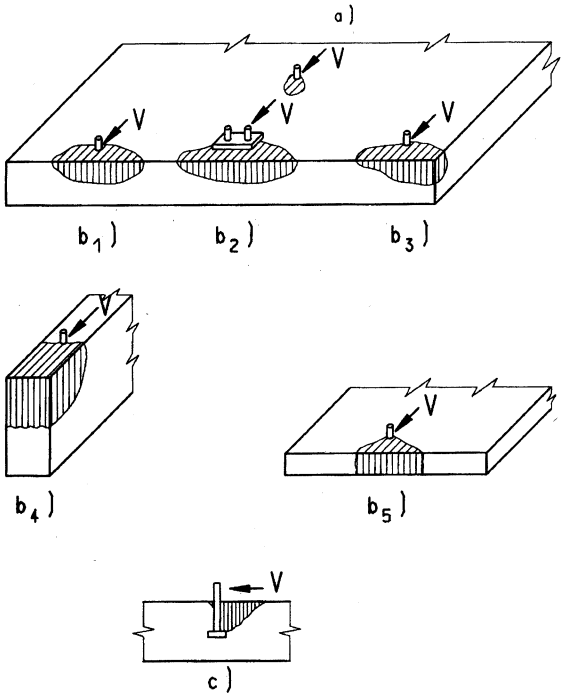

Fig. 5—Failure modes for fastenings under shear loading: (a) steel failure preceded by concrete spall; (b) concrete breakout; (c) concrete pryout failure for fastenings far from edge

[Fig. 2(d)]. This type of failure can be avoided by specifying minimum values of center-to-center and edge spacings, as well as component thickness. Again, prequalification testing under ASTM ZXXX[1] is designed to preclude such failures.

Concrete breakout failure [Fig. 2(b_1) through 2(b_3)] is a very important practical design case, because many fasteners are made such that a concrete failure will occur before yielding of steel. In fasteners with deeper embedment but thinner side cover, concrete blowout [Fig. 2(b_4)] can govern.[2] This latter case is not covered in this paper.

BEHAVIOR UNDER SHEAR LOADING

The failure modes of anchors loaded in shear are shown in Fig. 5. In principle, the same behavior as that under tensile loading can be observed. However, a pullout failure may theoretically occur only if the ratio of anchorage depth to anchor diameter is very small and the tensile capacity is very low. In contrast, in shear, a brittle concrete failure will occur for fastenings located close to the edge [Fig. 5(b)] and cannot be avoided by increasing anchorage depth. Steel failure, often proceeded by a local concrete spall in front of the anchor [Fig. 5(a)], will be observed for fasteners sufficiently far away from the edge. For that case, the load-displacement behavior will depend on ductility of the anchor steel. A concrete pryout-type failure of fastenings located quite far away from the edge [Fig. 5(c)] may occur for single anchors and especially for groups of anchors with a small ratio of embedment depth to anchor diameter and high tensile capacity.[3] The critical ratio depends on the anchor strength, concrete strength, and number and spacing of fasteners. This failure mode is not covered in this paper.

In practice, many fastenings or attachments are placed on a grout bed. For this type of installation, a grout failure may occur before any other type of failure. In this case, the shear load must be transferred into the base by bending the anchors. This may reduce the load transfer capacity when compared to a fastening or attachment installed directly on the base material. The effect of the grout bed on load transfer capacity is not discussed in this paper.

SCOPE

The relevant literature contains several approaches for the calculation of concrete failure load in uncracked concrete. The most important examples are design recommendations of ACI Committee 349,[4] PCI design procedures that are somewhat similar to those of ACI 349,[5] and the concrete capacity design (CCD) method based on the so-called κ-method developed at the University of Stuttgart.[6-8] The CCD method provides a clear visual explanation of calculation of the κ-factors used in the κ-method. It combines the transparency (ease of visualization of a physical model, making it readily understood by designers for application) of the ACI 349 method, accuracy of the κ-method, and a user-friendly rectangular failure surface calculation procedure. A comparison of the CCD method with the κ-method is given in References 9 and 10. From this comparison, it is evident that the CCD and κ-methods predict almost identical failure loads.

In this paper, the provisions of ACI 349-85 and the CCD method to predict the fastening capacity of brittle (concrete breakout) failures in uncracked concrete are compared with a large number of test results. To facilitate direct comparison, the capacity reduction factor ϕ of ACI 349 and partial material safety factor γ_m of the CCD method are both taken as 1.0. The comparison is made for fastenings both under tension load (single fasteners close to and far from the edge, as well as anchor groups with up to 36 fasteners far from the edge) and under shear load toward the edge (single fasteners and double fastenings installed close to the edge in wide and narrow as well as thick and thin members). Based on this comparison, the accuracy of the two design approaches is determined.

RESEARCH SIGNIFICANCE

While ductility is highly desirable in applications where there are substantial life safety concerns, a brittle failure mode covered by a sufficient safety factor is often acceptable. In both cases, concrete capacity must be predicted as accurately as possible to insure a ductile failure (ductile design) or sufficiently low probability of failure (brittle design), respectively. In many applications, the relevant design methods (ACI 349-85 and CCD method) will predict rather different concrete capacities. Therefore, screening of both methods based on an extensive data base is needed. Comparable earlier studies[11,12] are based on a small number of test data and did not include the newly developed CCD method.

DESIGN PROCEDURES

Fig. 6 shows concrete breakout cones for single anchors under tension or shear load, respectively, idealized according to ACI 349.[4] From this figure, it is evident that the concrete cone failure load depends on tensile capacity of the

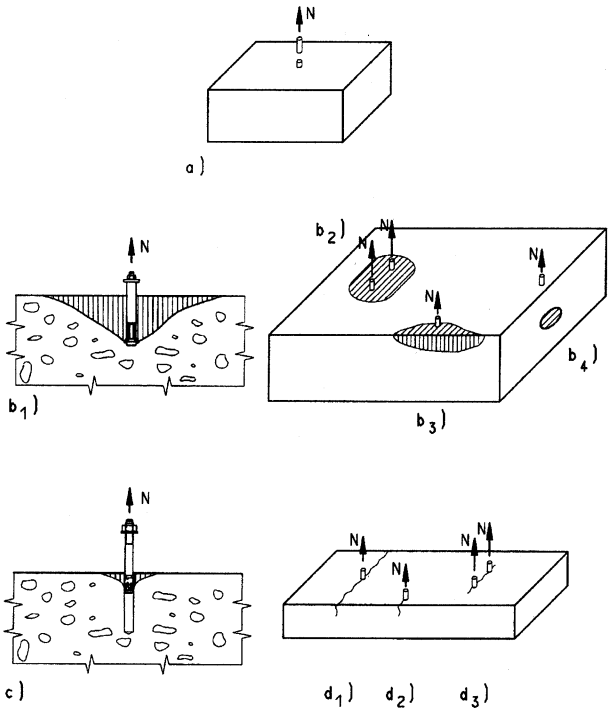

Fig. 2—Failure modes for fastenings under tensile loading: (a) steel failure; (b) concrete breakout; (c) pullout; (d) concrete splitting

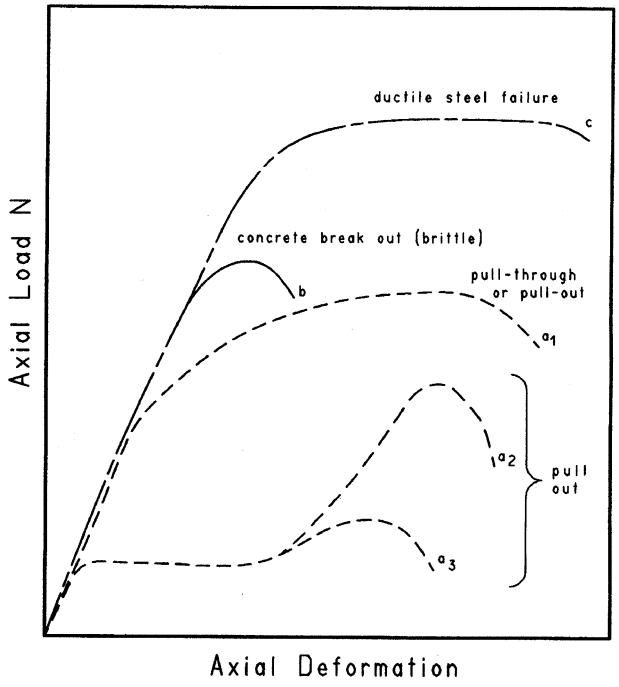

Fig. 3—Idealized load-deformation curves for fasteners under tension load

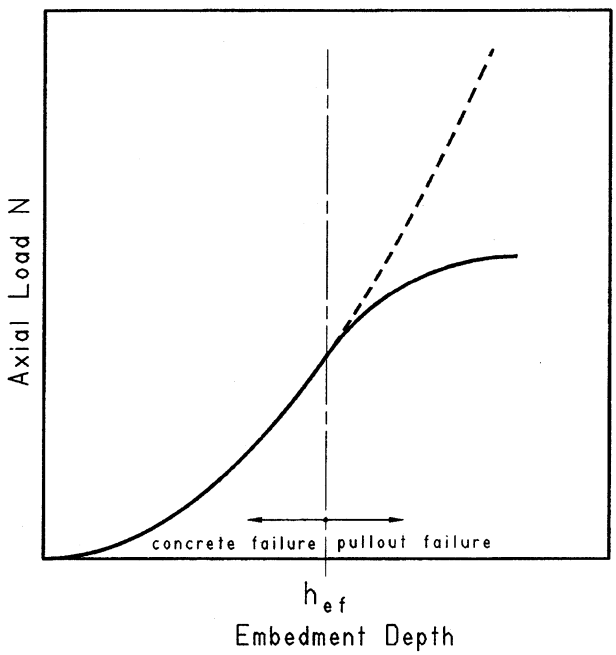

Fig. 4—Role of effective depth h_{ef} *for expansion anchors*

as those proposed in ASTM ZXXX.[1] In the case of a pull-through failure, in general the load-displacement relationship continuously increases and failure occurs at relatively large displacements (Line a_1 in Fig. 3). This anchor behavior is mainly dependent on the quality of the anchor production, and is acceptable in many applications.

In contrast, in the case of a pullout failure, the load-displacement curve may increase continuously until peak load (Line a_1 in Fig. 3) or the anchor may slip significantly in the hole at a load level larger than the remaining prestressing force of the anchor (Lines a_2 and a_3 in Fig. 3) before expanding further and developing a higher load capacity. This behavior is influenced considerably by the installation procedure and is highly undesirable. It must be prohibited by performance requirements in prequalification testing of the fastening device.

With expansion anchors, the depth of embedment can control the type of failure. As shown in Fig. 4, there is a critical embedment depth later termed h_{ef}, the effective embedment depth, at which the mode of failure changes from concrete failure to pullout. This depends on the expansion mechanism and h_{ef} is determined in prequalification tests.

The concrete bearing area of undercut anchors and headed studs is usually large enough to prevent pullout failure.

Ductile failures are failure by yielding of the fastening device or system fastened to the concrete before any breakout of concrete occurs [Fig. 2(a)].

Under conditions that the steel material is sufficiently ductile and the length of the fastener or attachment over which inelastic steel strains appear is large enough, and assuming that the concrete base material does not fail, a ductile steel failure will occur (Line c in Fig. 3).

Brittle failures are failure by concrete breakout or splitting of the structural concrete member before yielding of the fastener or fastened element [Fig. 2(b) and (d)] or by steel failure when the length over which inelastic steel strains appear is rather small.

For nonductile fasteners and cases where the concrete capacity is less than the fastener device capacity, a brittle failure will occur (Line b in Fig. 3).

It is not yet possible to determine theoretically the failure load to be expected in the "splitting" type of failure

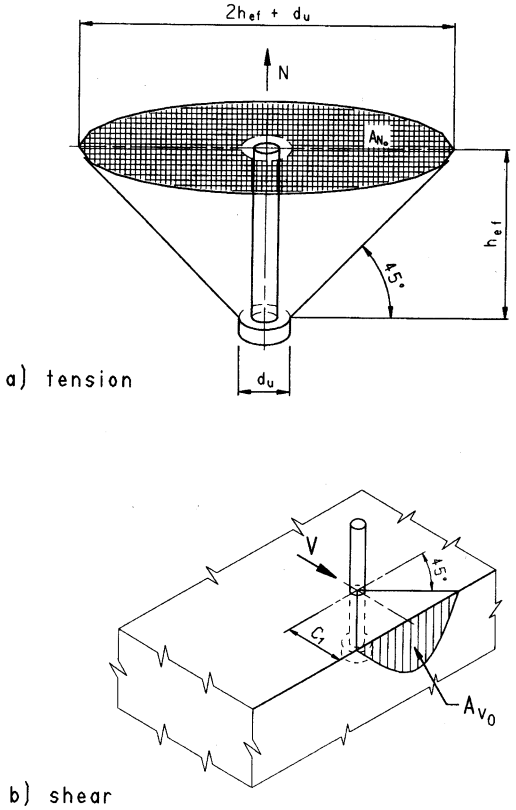

Fig. 6—Concrete breakout bodies idealized according to ACI 349: (a) tensile loading; (b) shear loading

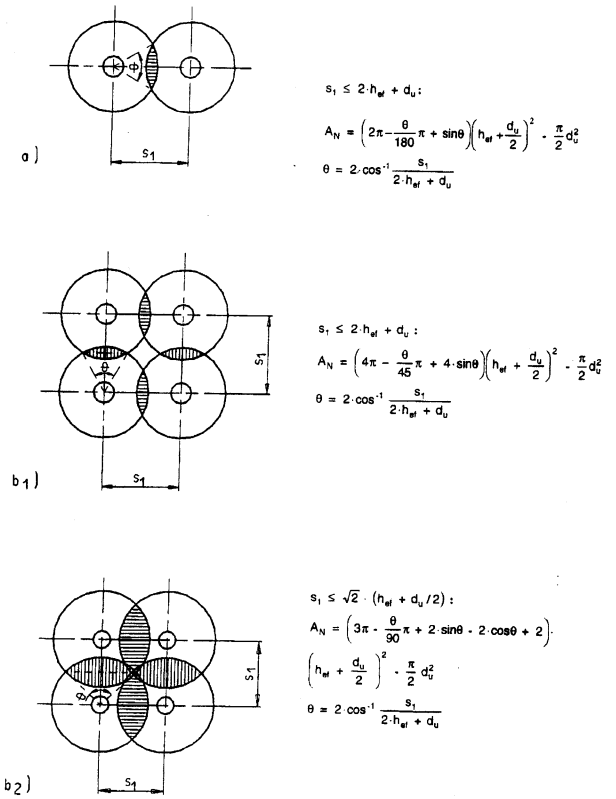

Fig. 7—Projected areas for multiple fastenings under tensile loading according to ACI 349: (a) double fastening; (b) quadruple fastening

concrete, considered throughout this paper to be proportional to $\sqrt{f_c'}$ or $\sqrt{f_{cc}'}$. Both design procedures predict average or mean failure loads, N_n or V_n. In subsequent codification of the CCD procedure for consideration by ACI Committee 318,[13] equations are based on the 5 percent fractile to provide part of the safety requirement. In addition, the codification proposal bases the equations on the strength of anchors in cracked concrete, with a multiplier that increases the capacity when used in uncracked concrete. This paper presents the results for uncracked concrete only and should be compared with design expressions for uncracked concrete. The behavior of anchor groups is infuenced by stiffness of the base plate. In this paper, a rigid base plate is presumed and no plastic action of the anchor group is considered.

ACI 349-85 tension loads

ACI Committee 349 is concerned with nuclear-related structures. Because of concern with nuclear safety, the philosophy of ACI 349 is to design ductile fastenings. To obtain a limit to guard against brittle concrete failure, the cone model was developed.[4,14,15]

Under tension loading, the concrete capacity of an arbitrary fastening is calculated assuming a constant tensile stress equal to $\phi \cdot 4 \cdot \sqrt{f_c'}$ acting on the projected area of the failure cone, taking the inclination between the failure surface and concrete surface as 45 deg

$$N_n = f_{ct} \cdot A_N \quad (1)$$

with

f_{ct} = $\phi \cdot 4 \cdot \sqrt{f_c'}$

ϕ = capacity reduction factor, here taken as 1.0

A_N = actual projected area of stress cones radiating toward attachment from bearing edge of anchors. Effective area shall be limited by overlapping stress cones, intersection of cones with concrete surfaces, bearing area of anchor heads, and overall thickness of concrete member

In the following, it is assumed that member thickness is sufficiently large to avoid any reduction of the concrete cone failure load.

For a single anchor unlimited by edge influences or overlapping cones [Fig. 6(a)]

$$N_{no} = (4 \cdot \sqrt{f_c'})\, A_{No}, \quad \text{lb} \quad (2)$$

with

A_{No} = projected area of a single anchor

= $\pi \cdot h_{ef}^2 (1 + d_u/h_{ef})$

The SI equivalent of Eq. (2) was determined assuming that

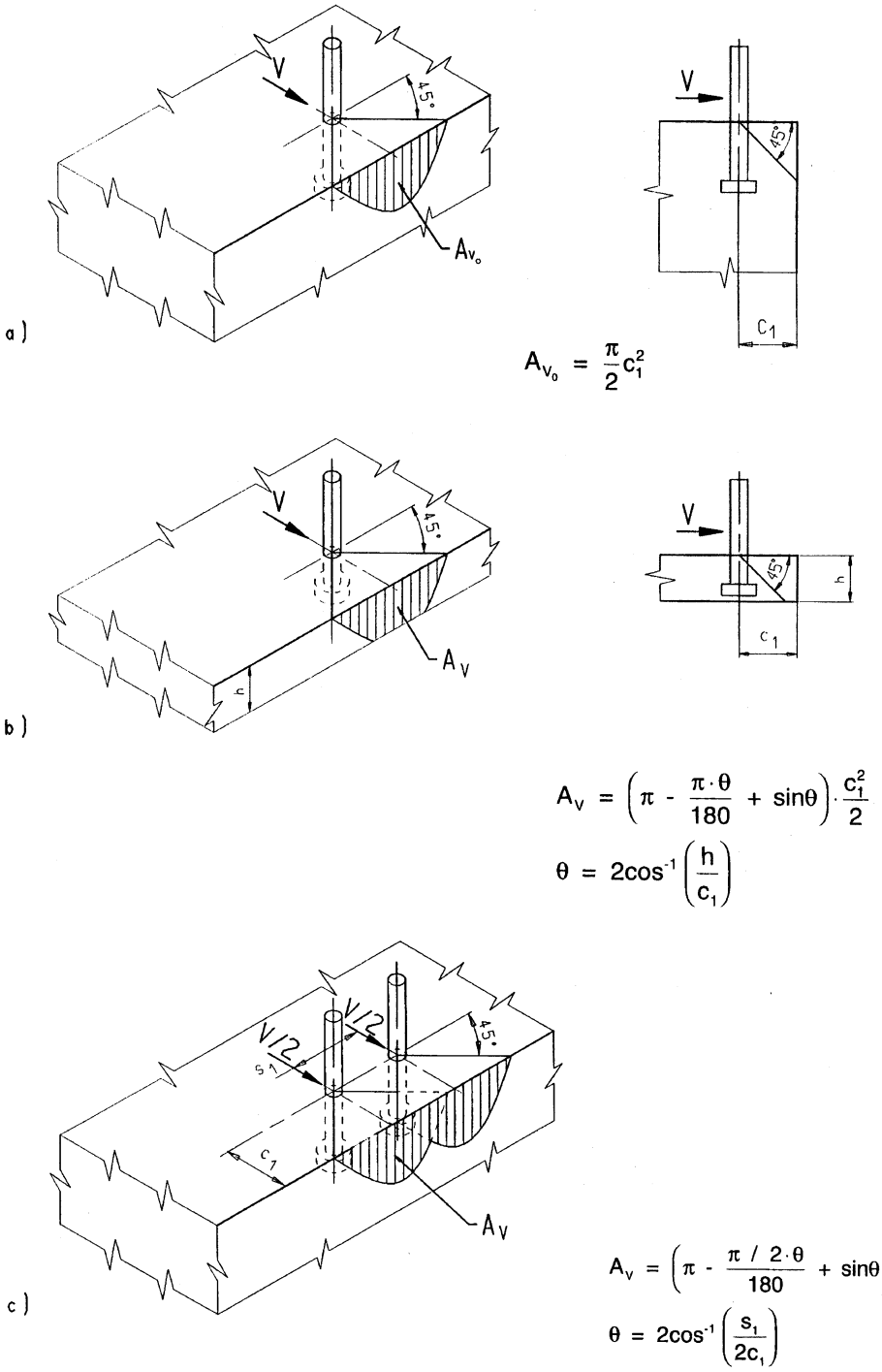

Fig. 8—Projected areas for fastenings under shear loading according to ACI 349: (a) single fastening installed in thick concrete member; (b) single fastening installed in thin concrete member ($h \le c_1$); (b) double fastening installed in thick concrete member ($s_1 < 2c_1$)

1 in. = 25.4 mm, 1 psi = 0.006895 N/mm^2, 1 lb = 4.448 N, and $\sqrt{f_{cc}'} = 1.18\sqrt{f_c'}$

$$N_{no} = 0.96 \cdot \sqrt{f_{cc}'} \cdot h_{ef}^2 \cdot \left(1 + \frac{d_u}{h_{ef}}\right), \quad N \tag{3}$$

For fastenings with edge effects ($c < h_{ef}$) and/or affected by other concrete breakout cones ($s < 2 \cdot h_{ef}$), the average failure load follows from Eq. (4)

$$N_n = \frac{A_N}{A_{No}} \cdot 4\sqrt{f_c'} \cdot \pi \cdot h_{ef}^2 \left(1 + \frac{d_u}{h_{ef}}\right), \quad lb \tag{4a}$$

$$= \frac{A_N}{A_{No}} \cdot N_{no\,[Eq\,(2)]}, \text{ lb} \tag{4b}$$

To obtain the failure load in SI units (N), Eq. (3) may be used in place of Eq. (2) in Eq. (4b).

Fig. 7 shows the determination of the projected areas A_N for double and quadruple fastenings. Note the computational complexity of determining Θ and A_N.

ACI 349-85 shear loads

The shear capacity of an individual anchor failing the concrete (Fig. 8), provided that the concrete half-cone is fully developed, is

$$V_{no} = \phi \cdot 4\sqrt{f_c'} \cdot \frac{\pi}{2} c_1^2, \quad \text{lb} \tag{5}$$

Again, with $\phi = 1$ and the conversion factors given, the SI equivalent is

$$V_{no} = \left((0.48 \cdot \sqrt{f_{cc}'}) c_1^2 \right), \quad \text{N} \tag{6}$$

If the depth of the concrete member is small ($h < c_1$) and/or the spacing is close ($s < 2 \cdot c_1$) and/or the edge distance perpendicular to the load direction is small ($c_2 < c_1$), then the load has to be reduced with the aid of the projected areas on the side of the concrete member

$$V_n = A_V \cdot 4 \cdot \sqrt{f_c'}, \quad \text{lb}$$

$$= \frac{A_V}{A_{Vo}} \cdot 4 \cdot \sqrt{f_c'} \cdot \frac{\pi}{2} \cdot c_1^2 \tag{7a}$$

$$= \frac{A_V}{A_{Vo}} \cdot V_{no,\,[\text{Eq. (5)}]}, \quad \text{lb} \tag{7b}$$

where

A_V = actual projected area

A_{Vo} = projected area of one fastener unlimited by edge influences, cone overlapping, or member thickness [Fig. 8(a)]

$= \pi/2 \cdot c_1^2$

To obtain the failure load in SI units (N), Eq. (6) may be used in place of Eq. (5) in Eq. 7(b).

Fig. 8 shows the determination of the projected areas A_V for shear loading using the cone concept of ACI 349. Again, the computations are complex for the examples shown in Fig. 8(b) and 8(c).

CCD method tension loads

The concrete capacity of arbitrary fastenings under tension or shear load can be calculated with the CCD method. To predict the steel capacity, additional design models are necessary, such as the one proposed in Reference 8 for elastic design of ductile and nonductile fasteners, or in Reference 16 for plastic design of ductile multiple fastenings. Note that failure load of anchors by pullout is lower than the concrete breakout capacity. Equations for calculation of pullout capacity are available but are not sufficiently accurate or general. Therefore, the pullout failure loads must be evaluated and regulated by prequalification testing.

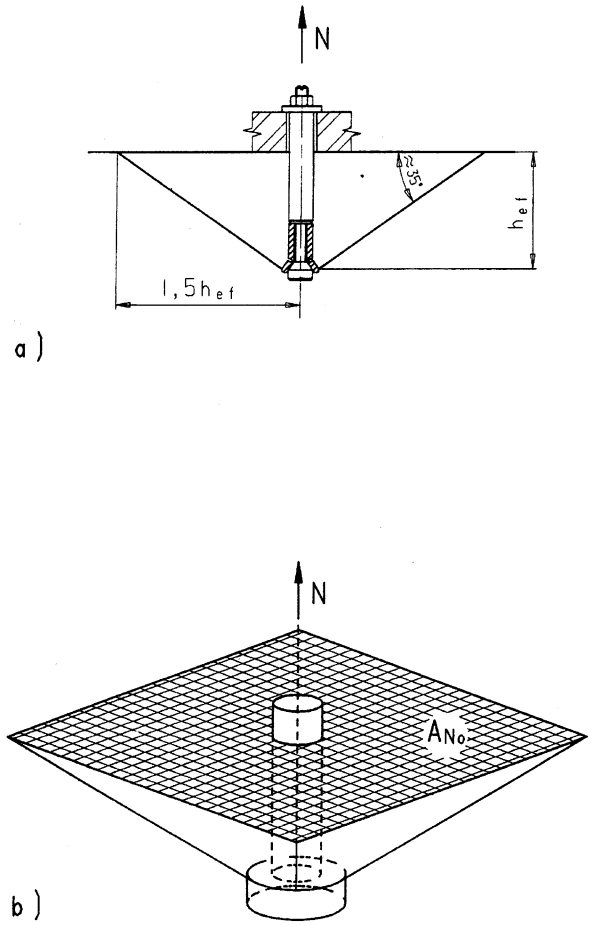

Fig. 9—Idealized concrete cone for individual fastening under tensile loading after CCD method

Under tension loading, the concrete capacity of a single fastening is calculated assuming an inclination between the failure surface and surface of the concrete member of about 35 deg. This corresponds to widespread observations that the horizontal extent of the failure surface is about three times the effective embedment (Fig. 9).

The concrete cone failure load N_{no} of a single anchor in uncracked concrete unaffected by edge influences or overlapping cones of neighboring anchors loaded in tension is given by Eq. (8)

$$N_{no} = k_1 \cdot \sqrt{f_c'} \cdot k_2 \cdot h_{ef}^2 \cdot k_3 \cdot h_{ef}^{-0.5} \tag{8}$$

where k_1, k_2, k_3 are calibration factors, with

$$k_{nc} = k_1 \cdot k_2 \cdot k_3$$

$$N_{no} = k_{nc} \cdot \sqrt{f_c'} \cdot h_{ef}^{1.5}, \quad \text{lb} \tag{9a}$$

where

k_{nc} = 35, post-installed fasteners

k_{nc} = 40, cast-in situ headed studs and headed anchor bolts

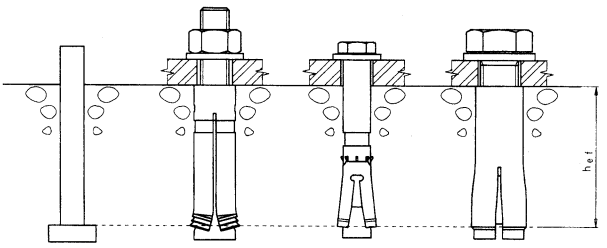

Fig. 10—Definition of effective anchorage depth h_{ef} *for different fastening systems*

$\sqrt{f_c'}$ = concrete compression strength measured on 6 by 12-in. cylinders, psi

h_{ef} = effective embedment depth, in. (Fig. 10)

In SI units, Eq. (9a) becomes

$$N_{no} = k_{nc} \cdot \sqrt{f_{cc}'} \cdot h_{ef}^{1.5}, \quad \text{N} \tag{9b}$$

where

k_{nc} = 13.5, post-installed fasteners

k_{nc} = 15.5, cast-in situ headed studs and headed anchor bolts

$\sqrt{f_{cc}'}$ = concrete compression strength measured on cubes with side length equal to 200 mm, N/mm^2

h_{ef} = effective embedment depth, mm (Fig. 10)

In Eq. (8), the factor $k_1 \cdot \sqrt{f_c'}$ represents the nominal concrete tensile stress at failure over the failure area, given by $k_2 \cdot h_{ef}^2$, and the factor $k_3/\sqrt{h_{ef}}$ gives the so-called size effect. Note that, by basing the tensile failure load on the effective embedment depth h_{ef}, the computed load will always be conservative, even for an anchor that might experience pullout, as shown in Fig. 4.

Fracture mechanics theory[17] indicates that in the case of concrete tensile failure with increasing member size, the failure load increases less than the available failure surface; that means the nominal stress at failure (peak load divided by failure area) decreases. This size effect is not unique to fastenings but has been observed for all concrete members with a strain gradient. For instance, it is well known that the bending strength of unreinforced concrete beams and shear strength of beams and slabs without shear reinforcement decrease with increasing member depth. Size effect has been verified for fastenings by experimental and theoretical investigations.[8,18-20] A more detailed explanation of the application of Bažant's theory to fastenings is given in Reference 21. Since the aggregate size in the test specimens is not specifically introduced into the CCD method, an approximation is used. Since strain gradient in concrete for fastenings is very large, size effect is maximum and very close to the linear elastic fracture mechanics solution. Therefore, the nominal stress at failure decreases in proportion to $1/\sqrt{h_{ef}}$ and the failure load increases with $h_{ef}^{1.5}$.

Higher coefficients for headed studs and headed anchor bolts in Eq. (9) are valid only if the bearing area of headed studs and anchors is so large that concrete pressure under the head is $\leq 13\sqrt{f_c'}$ at failure.[8] Because the concrete pressure under the head of most currently available post-installed undercut anchors exceeds $13f_c'$ at failure, $k_{nc} = 35$ or 13.5 (SI) is recommended for use with this and other post-installed anchors.

In certain cases, when deeper embedments are used with relatively thin edge cover, there is a chance of a side-face blowout failure at a significantly reduced load. Such cases are not covered in this paper.

If fastenings are located so close to an edge that there is not enough space for a complete concrete cone to develop, the load-bearing capacity of the anchorage is also reduced. This is also true for fasteners spaced so closely that the breakout cones overlap. One of the principal advantages of the CCD method is that calculation of the changes in capacity due to factors such as edge distance, spacing, geometric arrangement of groupings, and similar variations can be readily determined through use of relatively simple geometrical relationships based on rectangular prisms. The concrete capacity can be easily calculated according to Eq. (10)

$$N_n = \frac{A_N}{A_{No}} \cdot \psi_2 \cdot k_{nc} \cdot \sqrt{f_c'} \cdot h_{ef}^{1.5} \tag{10a}$$

$$N_n = \frac{A_N}{A_{No}} \cdot \psi_2 \cdot N_{no} \tag{10b}$$

where

A_{No} = projected area of one anchor at the concrete surface unlimited by edge influences or neighboring anchors, idealizing the failure cone as a pyramid with a base length $s_{cr} = 3h_{ef}$ [Fig. 11(a)]

= $9 \cdot h_{ef}^2$

A_N = actual projected area at the concrete surface, assuming the failure surface of the individual anchors as a pyramid with a base length $s_{cr} = 3h_{ef}$. For examples, see Fig. 11(b) through (d)

ψ_2 = tuning factor to consider disturbance of the radial symmetric stress distribution caused by an edge, valid for anchors located away from edges

$$\psi_2 = 1 \text{ if } c_1 \geq 1.5h_{ef} \tag{10c}$$

$$\psi_2 = 0.7 + 0.3\frac{c_1}{1.5h_{ef}} \text{ if } c_1 \leq 1.5h_{ef} \tag{10d}$$

where

c_1 = edge distance to the closest edge. (Note that symbols for ψ_1, ψ_2, ψ_4, and ψ_5 and the order in which they appear in this text were selected to agree with Reference 13.)

k_{nc} = see Eq. (9)

N_{no} = concrete cone failure load of one anchor unaffected by edge or overlapping stress cones acording to Eq. (9)

h_{ef} = effective anchorage depth (Fig. 10). For fastenings with three or four edges and $c_{max} \le 1.5h_{ef}$ (c_{max} = largest edge distance), the embedment depth to be inserted in Eq. (10a) and (10b) is limited to $h_{ef} = c_{max}/1.5$. This gives a constant failure load for deep embedments[22]

Examples for calculation of projected areas are given in Fig. 11. Note the relatively simple calculation for the CCD method compared to Fig. 7 illustrating the ACI 349 method.

In Eq. (10), it is assumed that the failure load is linearly proportional to the projected area. This is taken into account by the factor A_N/A_{No}. For fastenings close to an edge, the axisymmetric state of stress, which exists in concrete in the case of fastenings located far from the edge, will be disturbed by the edge. Due to this disturbance, the concrete cone failure load will be reduced. (This also occurs in cracked concrete.[8,23]) This is taken into account by the tuning factor ψ_2. A linear reduction from $\psi_2 = 1.0$ for $c_1 \ge 1.5h_{ef}$ (no edge influence) to $\psi_2 = 0.7$ for the theoretical case $c_1 = 0$ has been assumed.

Up to this point, it has been assumed that anchor groups are loaded concentrically in tension. However, if the load acts eccentrically on the anchor plate, it is not shared equally by all fasteners. Based on a proposal in Reference 24, this effect can be taken into account by an additional factor ψ_1 [Eq. (11)]

$$N_n = \frac{A_N}{A_{No}} \cdot \psi_1 \cdot \psi_2 \cdot N_{no} \qquad (11a)$$

with A_N, A_{No}, ψ_2, and N_{no} as defined in Eq. (10).

ψ_1 = factor taking into account the eccentricity of the resultant tensile force on tensioned fasteners. In the case where eccentric loading exists about two axes (Fig. 11), the modification factor ψ_1 shall be computed for each axis individually and the product of the factors used as ψ_1 in Eq. (11a)

$$= \frac{1}{1 + 2e_N'/(3h_{ef})} \le 1 \qquad (11b)$$

e_N' = distance between the resultant tensile force of tensioned fasteners of a group and centroid of tensioned fasteners (Fig. 12)

Fig. 12 shows examples of an eccentricaly loaded quadruple fastening under tensile loading located close to a corner. In Fig. 13, Eq. (11a) is applied for the case of a double fastening. In this figure (as in Fig. 12), it is assumed that the eccentricity e_N' of the resultant tension force on the fasteners is equal to eccentricity e_N of the applied load. This is valid for $e_N \le s_t/6$ and for $e_N > s_t/6$ if the fastener displacements are neglected. If the load acts concentrically on the anchor plate, Eq. (10) is valid ($\psi_1 = 1$) [Fig. 13(a)]. If only one fastener is loaded [Fig. 13(c)], the failure load of the group is equal to the concrete capacity of one fastener without spacing effects. For $0 \le e_N' \le 0.5s_t$, a nonlinear

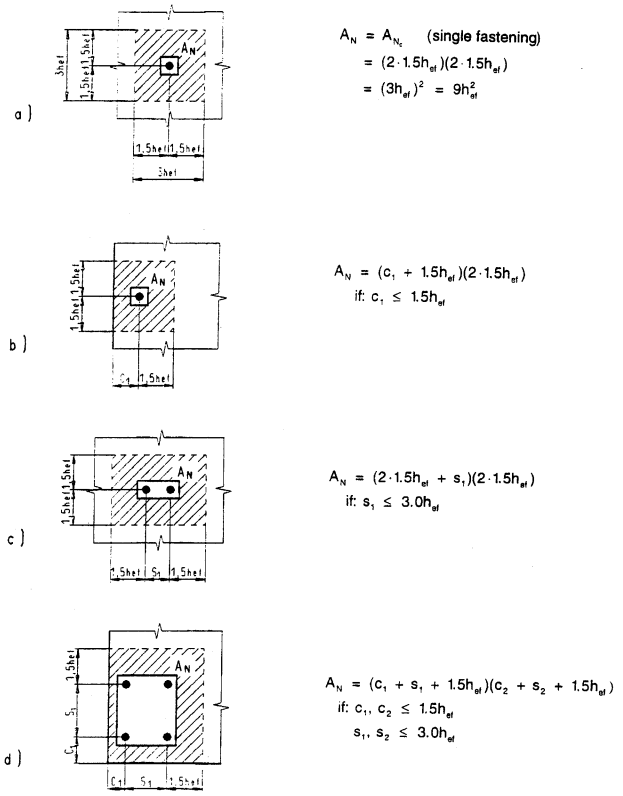

Fig. 11—Projected areas for different fastenings under tensile loading according to CCD method

relationship of the concrete capacity is proposed between these limiting cases (Fig. 14).

CCD method shear loads

The concrete capacity of an individual anchor in a thick uncracked structural member under shear loading toward the free edge (Fig. 15) is

$$V_{no} = 13\,(1/d_o)^{0.2}\sqrt{d_o} \cdot \sqrt{f_c'} \cdot c_1^{1.5}\ \text{, lb} \qquad (12a)$$

where

d_o = outside diameter of fastener, in.

l = activated load-bearing length of fastener, in., $\le 8d_o$ (Reference 25)

= h_{ef} for fasteners with a constant overall stiffness, such as headed studs, undercut anchors, and torque-controlled expansion anchors, where there is no distance sleeve or the expansion sleeve also has the function of the distance sleeve

= $2d_o$ for torque-controlled expansion anchors with distance sleeve separated from the expansion sleeve

c_1 = edge distance in loading direction, in.

In SI units with length quantities in mm and stress in N/mm^2, this equation becomes

$$V_{no} = 1/d_o^{0.2}\sqrt{d_o} \cdot \sqrt{f_{cc}'} \cdot c_1^{1.5} \qquad (12b)$$

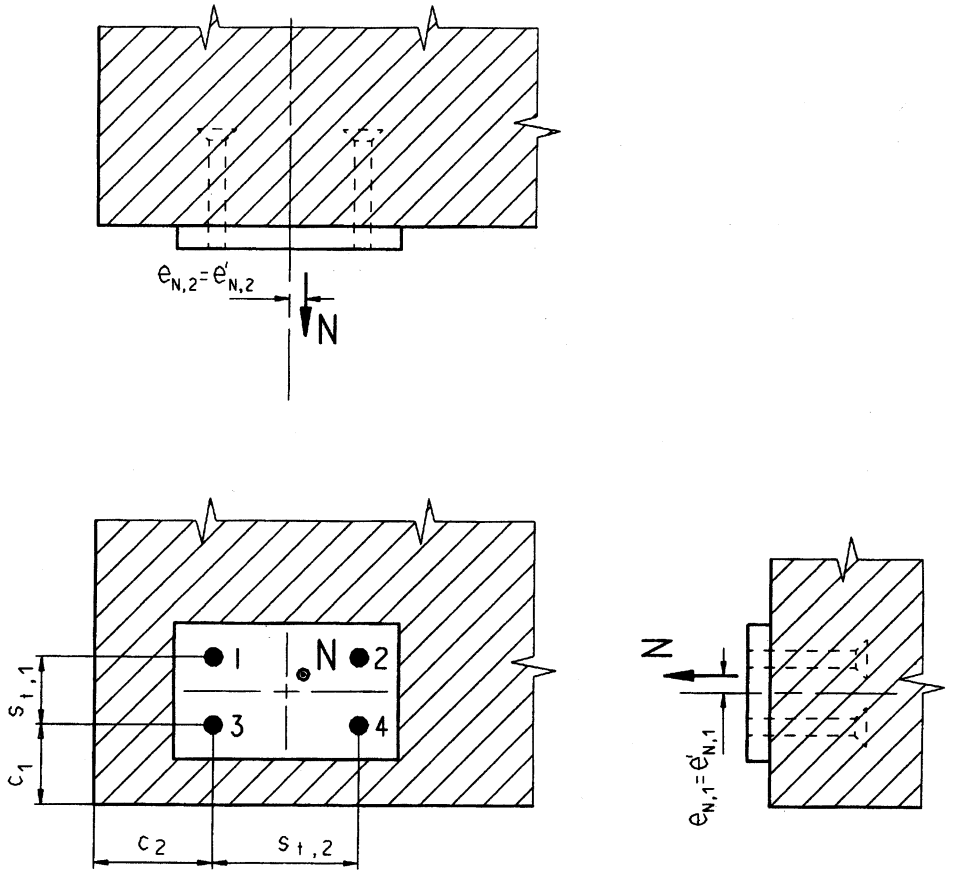

Fig. 12—Examples of eccentrically loaded quadruple fastening under tensile loading located close to corner

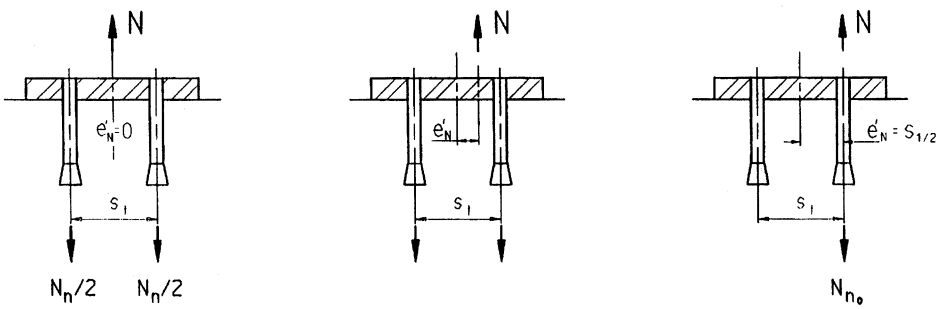

$$N_n = \frac{A_n}{A_{n_0}} \cdot N_{n_0}$$

a)

$$N_n = \frac{A_N}{A_{N_0}} \cdot \psi_1 \cdot N_{n_0}$$

$$\psi_1 = \frac{1}{1 + 2e'_N / (3h_{ef})}$$

b)

$$N_n = N_{n_0}$$

c)

Fig. 13—Effect of eccentricity of tensile force on failure load of double fastening[24]

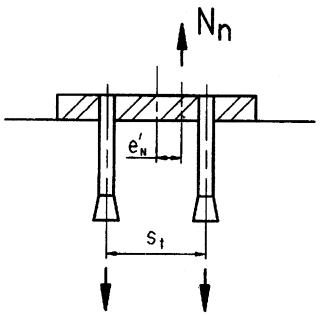

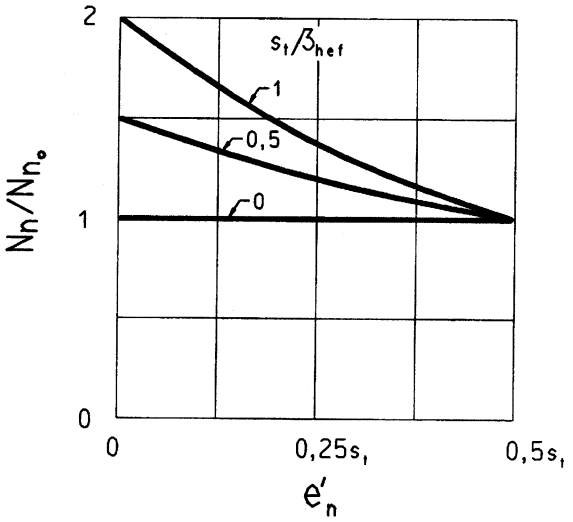

Fig. 14—Influence of eccentricity of tensile force on failure load of double fastening[24]

According to Eq. (12), the shear failure load does not increase with the failure surface area, which is proportional to c_1^2. Rather, it is proportional to $c_1^{1.5}$. This is again due to size effect. Furthermore, the failure load is influenced by the anchor stiffness and diameter. The size effect on the shear failure load has been verified theoretically and experimentally.[26]

The shear load capacity of single anchors and anchor groups loaded toward the edge can be evaluated from Eq. (13a) in the same general manner as for tension loading by taking into account that the size of the failure cone is dependent on the edge distance in the loading direction, while in tension loading it is dependent on the anchorage depth (Fig. 16)

$$V_n = \frac{A_v}{A_{vo}} \cdot \psi_4 \cdot \psi_5 \cdot V_{no} \qquad (13a)$$

where

A_v = actual projected area at side of concrete member, idealizing the shape of the fracture area of individ-

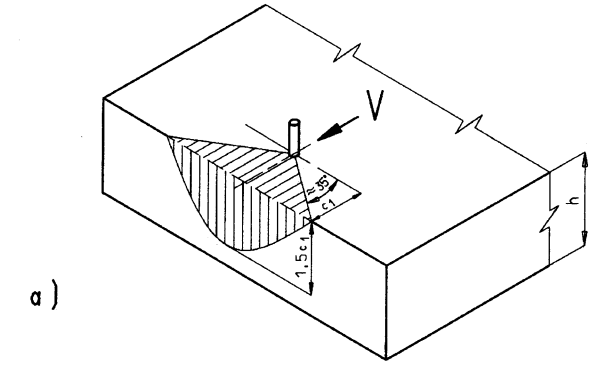

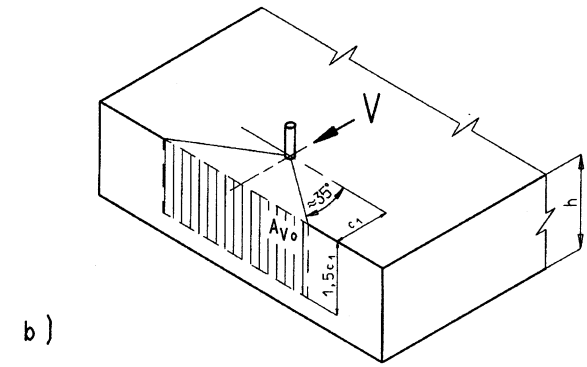

Fig. 15—Concrete failure cone for individual fastener in thick concrete member under shear loading toward edge: (a) from test results; (b) simplified design model according to CCD method

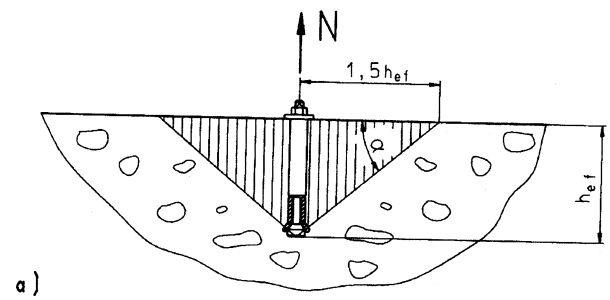

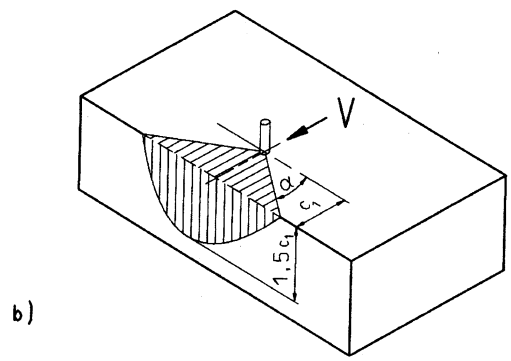

Fig. 16—Comparison of tension and shear loading for CCD method

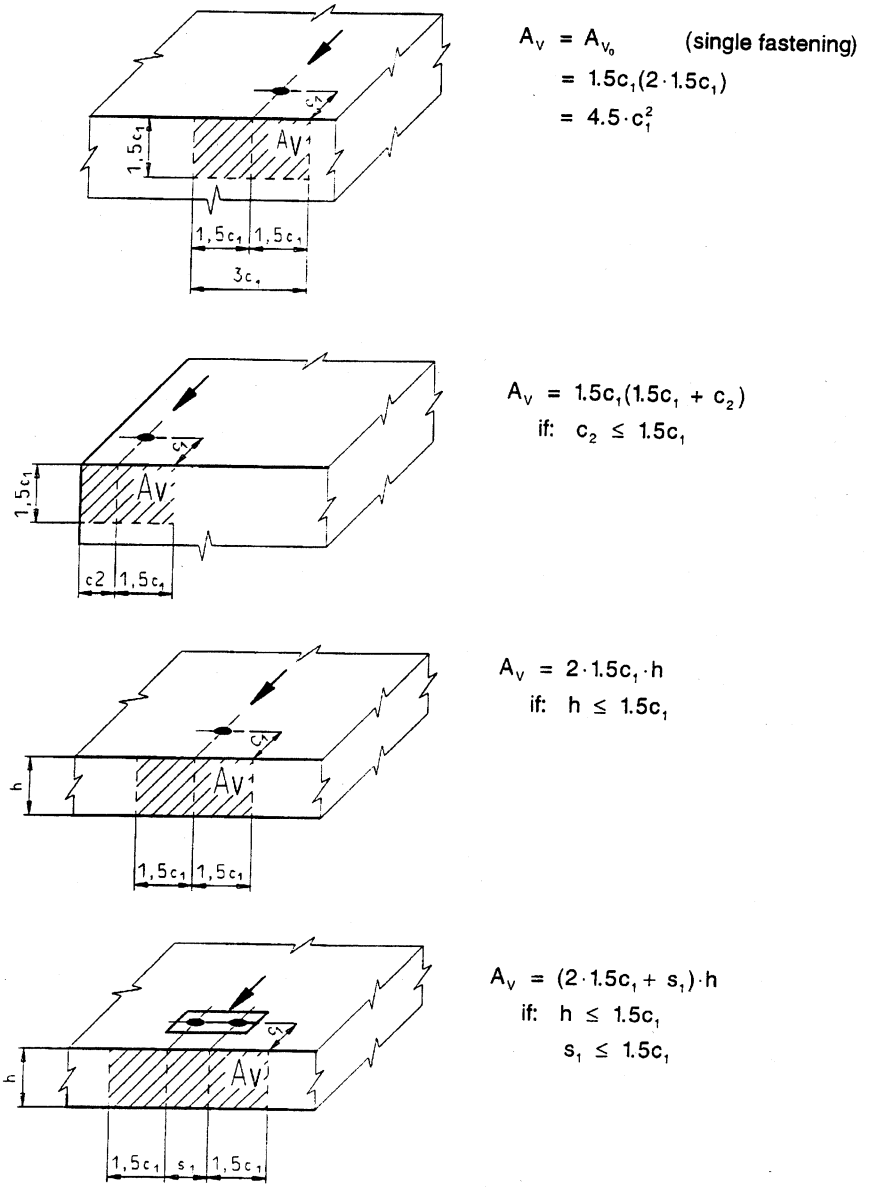

Fig. 17—Projected areas for different fastenings under shear loading according to CCD method

ual anchors as a half-pyramid with side length $1.5c_1$ and $3c_1$ (Fig. 17)

A_{vo} = projected area of one fastener unlimited by corner influences, spacing, or member thickness, idealizing the shape of the fracture area as a half-pyramid with side length $1.5c_1$ and $3c_1$ [Fig. 15(b) and 17(a)]

ψ_4 = effect of eccentricity of shear load

$$= \frac{1}{1 + 2e_v'/(3_{c1})} \qquad (13b)$$

e_v' = distance between resultant shear force of fasteners of group resisting shear and centroid of sheared fasteners (Fig. 18)

ψ_5 = tuning factor considering disturbance of symmetric stress distribution caused by a corner

$$\psi_5 = 1 \quad \text{if} \quad c_2 \ge 1.5c_1$$

$$\psi_5 = 0.7 + 0.3 \cdot \frac{c_2}{1.5c_1} \quad \text{if} \quad c_2 \le 1.5c_1 \qquad (13c)$$

c_1 = edge distance in loading direction, in. (Fig. 17); for fastenings in a narrow, thin member with $c_{2,max} < 1.5c_1$ ($c_{2,max}$ = maximum value of edge distances perpendicular to the loading direction) and $h < 1.5c_1$, the edge distance to be inserted in Eq. (13a), (13b), and (13c) is limited to $c_1 = \max(c_{2,max}/1.5; h/1.5)$. This gives a constant failure load independent of the edge distance c_1 (Reference 21)

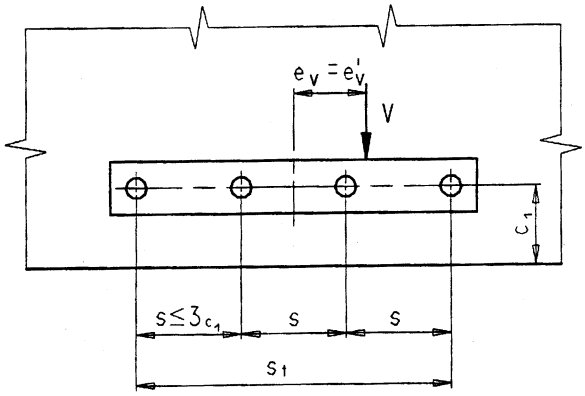

Fig. 18—Example of multiple fastening with cast-in situ headed studs close to edge under eccentric shear loading

c_2 = edge distance perpendicular to load direction (Fig. 17)

Examples for calculation of projected areas are shown in Fig. 17. Note the relatively simple calculation compared to the more complex geometry of the ACI 349 procedures illustrated in Fig. 8.

The considerations just presented relate to shear loads acting perpendicular to and toward the free edge [Fig. 19(a)]. If the load acts in a direction parallel to the edge [Fig. 19(b)], the test performed at TNO Delft[27] indicates that the shear load capable of being resisted is about twice as large as the load that can be resisted in the direction perpendicular to and toward the edge (Fig. 19). A similar value can be conservatively used for resistance to loads in the direction perpendicular to but away from the edge.[26]

Comparison of ACI 349 and CCD methods

The main differences between these design approaches are summarized in Table 1. They are as follows:

1. The way in which they consider influence of anchorage depth h_{ef} (tensile loading) and edge distance c_1 (shear loading).

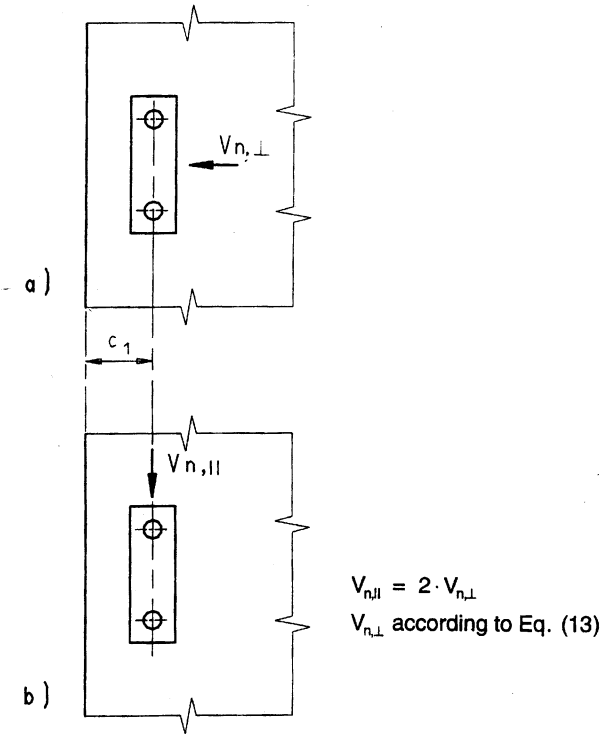

Fig. 19—Double fastening: (a) shear load perpendicular to edge; (b) shear load parallel to edge

2. The assumption of slope of the failure cone surface. This leads to different minimum spacings and edge distances to develop full anchor capacity.

3. The assumption about the shape of the fracture area (ACI 349: cone, CCD method: pyramid approximating an idealized cone). In both methods, the influence of edges and overlapping cones is taken into account by projected areas, based on circles (ACI 349) or rectangles (CCD method), respectively. Due to this, calculation of the projected area is rather simple in the case of the CCD method and often rather complicated in the case of ACI 349.

4. The CCD method takes into account disturbance of the stresses in concrete caused by edges and influence of load

Table 1—Comparison of the influence of main parameters on maximum load predicted by ACI 349 and CCD methods

		ACI 349-85	CCD method
Anchorage depth, tension		h_{ef}^2	$h_{ef}^{1.5}$
Edge distance, shear		c_1^2	$c_1^{1.5}$
Slope of failure cone		α = 45 deg	$\alpha \approx 35$ deg
Required spacing to develop full anchor capacity		$2h_{ef}$, tension $2c_1$, shear	$3h_{ef}$, tension $3c_1$, shear
Required edge distance to develop full anchor capacity		$1h_{ef}$, tension $1c_1$, shear	$1.5h_{ef}$, tension $1.5c_1$, shear
Small spacing or close to edge	1 direction	Nonlinear (area-proportional) reduction	Linear reduction
	2 directions		Nonlinear reduction
Eccentricity of load		—	Taken into account

Table 2—Single fastenings with post-installed fasteners far from edge, test series—Tensile loading

Edge spacing	Country of test	n	f'_{cc200}, N/mm^2			h_{ef}, mm		
			Minimum	Average	Maximum	Minimum	Average	Maximum
c_1 $1.5h_{ef}$	GB	55	23.0	27.5	34.0	22.0	59.2	136.0
	F	79	13.6	28.9	54.9	42.0	89.0	156.0
	S	28	16.3	29.8	43.7	32.0	55.9	125.0
	D	360	8.8	31.7	75.4	17.6	62.7	220.0
	EUR	522	8.8	30.8	75.4	17.6	65.9	220.0
	USA	88	15.3	33.1	52.0	24.5	69.0	275.0
	Σ	610	8.8	31.1	75.4	17.6	66.3	275.0
c_1 $1.0h_{ef}$	GB	58	23.0	27.1	34.0	22.0	63.2	136.0
	F	81	13.6	28.0	54.9	42.0	87.0	156.0
	S	28	16.3	29.8	43.7	32.0	55.9	125.0
	D	400	8.8	31.6	75.4	17.6	62.6	220.0
	EUR	567	8.8	30.7	75.4	17.6	65.1	220.0
	USA	92	15.3	32.6	52.0	24.5	67.6	275.0
	Σ	659	8.8	31.0	75.4	17.6	65.5	275.0

Table 3—Single fastenings with cast-in situ headed studs far from edge, single tests—Tensile loading

Edge spacing	Country of test	n	f'_{cc200}, N/mm^2			h_{ef}, mm		
			Minimum	Average	Maximum	Minimum	Average	Maximum
c_1 $1.5h_{ef}$	S	3	30.9	39.5	56.7	130.0	137.3	142.0
	CS	26	28.3	31.2	34.4	50.0	177.0	450.0
	D	192	11.4	28.5	71.9	42.9	156.4	525.0
	EUR	221	11.4	28.9	71.9	42.9	158.5	525.0
	USA	27	24.3	28.9	43.1	63.5	109.7	251.4
	Σ	248	11.4	28.9	71.9	42.9	152.6	525.0
c_1 $1.0h_{ef}$	S	6	30.9	38.6	56.7	112.0	133.3	142.0
	CS	26	28.3	31.2	34.4	50.0	177.0	450.0
	D	220	11.4	28.3	71.9	42.9	145.0	525.0
	EUR	252	11.4	28.8	71.9	42.9	147.0	525.0
	USA	28	24.3	29.3	43.1	63.5	107.9	251.4
	Σ	280	11.4	28.6	71.9	42.9	141.7	525.0

eccentricities. These influencing factors are neglected by ACI 349.

TEST DATA

In the following sections, some extracts of the data base are reproduced to give the reader a sense of the large number of test series, individual tests, and range of variables considered. The original summary of test results is given in Reference 10. Only tests where a concrete breakout failure occurred were taken into account. In response to review comments after submission of this paper for publication, data from the Prague tests reported by Eligehausen et al. [21] and the Arkansas Nuclear One tests[28] were added.

Tensile loading

Tables 2 through 5 give an overview of the number of tensile tests and range of the varied parameters. No difference in the procedure of performing tests with anchors under tensile loading between Europe and the U.S. could be discovered.

Shear loading

Tables 6 through 8 give an overview of the number of shear tests and range of the varied parameters.

In European tests with anchors under shear loading, a fluoropolymer sheet was always inserted between the concrete surface and steel plate. This is to simulate reduction in friction between the steel plate and concrete surface caused by reduction of the prestressing force with time[9] and by use of a plate with a relatively smooth surface (e.g., a painted, cold-drawn, or greased plate). In the U.S., tests are usually performed with an unpainted steel plate attached directly on the concrete surface with no fluoropolymer sheet in between. This increases friction resistance and causes the U.S. test values to be higher.

COMPARISON OF DESIGN METHODS WITH TEST DATA

In this section, test data from the wide range of tests shown in the previous section will be compared with the CCD and ACI design procedures.

Table 4—Single fastenings with post-installed fasteners close to edge, test series—Tensile loading

Edge spacing	Country of test	n	f'_{cc200}, N/mm^2			h_{ef}, mm			c_1, mm		
			Minimum	Average	Maximum	Minimum	Average	Maximum	Minimum	Average	Maximum
$c_1 \le 1.5\ h_{ef}$	GB	3	23.0	23.8	25.5	37.0	67.3	100.0	50.0	83.3	120.0
	F	2	18.4	18.4	18.4	63.5	63.5	63.5	63.5	63.5	63.5
	D	36	24.0	28.7	59.0	30.0	81.5	220.0	30.0	95.6	330.0
	EUR	41	18.4	27.9	59.0	30.0	79.6	220.0	30.0	93.1	330.0
	USA	42	17.2	27.1	34.1	34.2	118.0	222.3	31.8	96.0	177.8
	Σ	83	17.2	27.5	59.0	30.0	99.0	223.3	30.0	94.6	330.0
$c_1 \le 1.0\ h_{ef}$	D	10	24.0	26.3	37.7	53.0	100.9	220.0	30.0	93.5	220.0
	USA	30	18.6	27.7	34.1	34.2	137.8	222.3	31.8	100.8	158.8
	Σ	40	18.6	27.3	37.7	34.2	128.6	222.3	30.0	98.9	220.0

Table 5—Quadruple fastenings with cast-in situ headed studs, single tests—Tensile loading

Edge spacing	Country of test	n	f'_{cc200}, N/mm^2			h_{ef}, mm			c_1, mm			s, mm		
			Minimum	Average	Maximum	Minimum	Average	Maximum	Minimum	Average	Maximum	Minimum	Average	Maximum
Quadruple fastening	USA	3	32.5	33.6	35.8	161.9	161.9	161.9	—	—	—	50.8	76.2	101.6
	D	32	17.9	27.5	38.9	67.3	179.4	360.3	—	—	—	80.0	125.5	400.0
	Σ	35	17.9	28.1	38.9	67.3	177.9	360.3	—	—	—	50.8	146.0	400.0

Table 6—Single fastenings with post-installed fasteners and fully developed concrete breakout, test series—Shear loading

Country of test	n	f'_{cc200}, N/mm^2			h_{ef}, mm			d, mm			c_1, mm		
		Minimum	Average	Maximum	Minimum	Average	Maximum	Minimum	Average	Maximum	Minimum	Average	Maximum
USA	60	21.3	31.7	53.9	25.0	94.5	220.0	8.0	20.9	32.0	40.0	128.3	300.0
D	84	16.1	25.7	48.4	27.4	70.3	167.6	6.4	14.6	25.4	38.1	98.0	203.2
Σ	144	16.1	28.2	53.9	25.0	80.4	220.0	6.4	17.2	32.0	38.1	110.6	300.0

Table 7—Single fastenings with post-installed fasteners in concrete members with limited thickness, single tests—Shear loading

Country of test	n	f'_{cc200}, N/mm^2			h_{ef}, mm			d, mm			c_1, mm			c_2, mm		
		Minimum	Average	Maximum	Minimum	Average	Maximum	Minimum	Average	Maximum	Minimum	Average	Maximum	Minimum	Average	Maximum
D	38	35.2	42.8	46.4	155.0	250.8	306.0	20.0	27.5	40.0	63.0	140.2	220.0	62.5	184.1	300.0

Table 8—Double fastenings in thick concrete members, single tests

Anchorage device	Country of test	n	f'_{cc200}, N/mm^2			h_{ef}, mm			d, mm			c_1, mm			c_2, mm		
			Minimum	Average	Maximum	Minimum	Average	Maximum	Minimum	Average	Maximum	Minimum	Average	Maximum	Minimum	Average	Maximum
Expansion anchor	D	36	20.5	24.8	27.2	80.0	81.7	100.0	18.0	20.7	24.0	80.0	172.1	200.0	80.0	190.0	400.0

Tensile loading

In Fig. 20 and 21, measured failure loads of individual anchors are plotted as a function of embedment depth. The tests were performed on concrete with different compression strengths. Therefore, the measured failure loads were normalized to f'_{cc} = 25 N/mm^2 (f'_c = 3070 psi) by multiplying them with the factor $(25/f_{cc,\,test})^{0.5}$. In addition, predicted failure loads according to ACI and the CCD methods are plotted. As can be seen, the tension failure loads predicted by the CCD method compare rather well with the mean test results over the total range of embedment depths, with the exception of the two post-installed fasteners at the deepest embedment. In contrast, anchor strengths predicted by ACI 349 can be considered as a lower bound for shallow embedments and give quite unconservative results for the deepest embedded headed studs. This is probably due to the fact that size effect

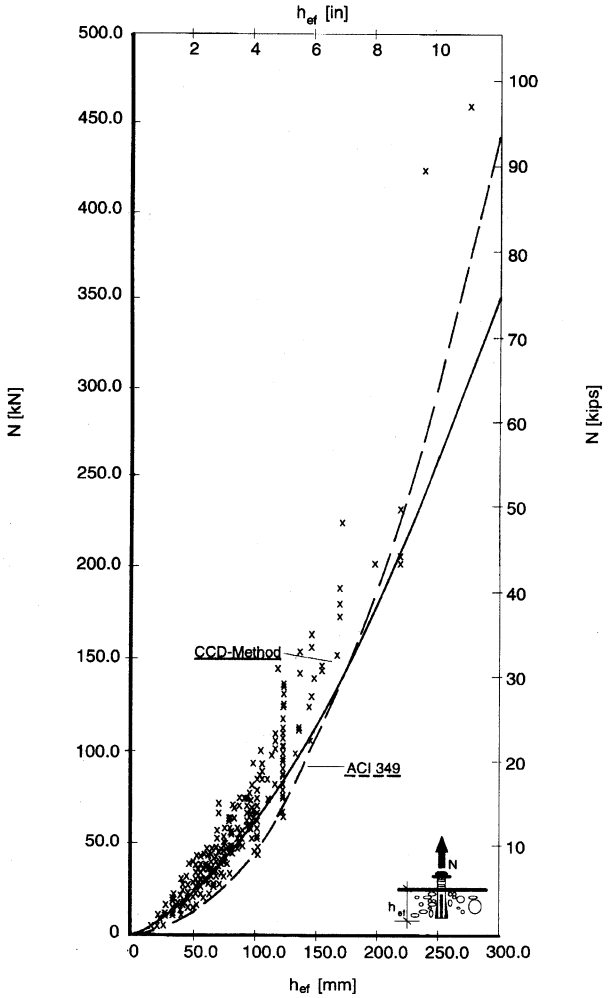

Fig. 20—Concrete breakout load for post-installed fasteners, unaffected by edges or spacing effects—Tensile test results and predictions

is neglected by ACI 349. Substantial scatter exists with the deep embedment data, justifying a conservative approach in this region.

Fig. 22 shows the results of all evaluations for tensile loading with post-installed fasteners far from the edge. Average values of the ratios $N_{u,test}$ to $N_{n,predicted}$ and corresponding coefficients of variation for both methods are plotted. The average and coefficient of variation are substantially better for the CCD method than for ACI 349. This is also true when the data are subdivided into five different anchor types (Fig. 23) and for headed studs without edge or spacing influences (Fig. 24). Eq. (9) uses the same coefficient k_{nc} for undercut anchors as for other post-installed anchors. The results shown in Fig. 23 support this procedure. These undercut anchor tests were typically for undercut anchors with head bearing pressures greater than $13f_c'$. Better values would be expected if the undercuts were proportioned for lower bearing pressures.

The coefficient of variation of the ratios of measured failure load to the value predicted by the CCD method is about 15 percent for headed studs and undercut anchors, which agrees with the coefficient of variation of the concrete tensile

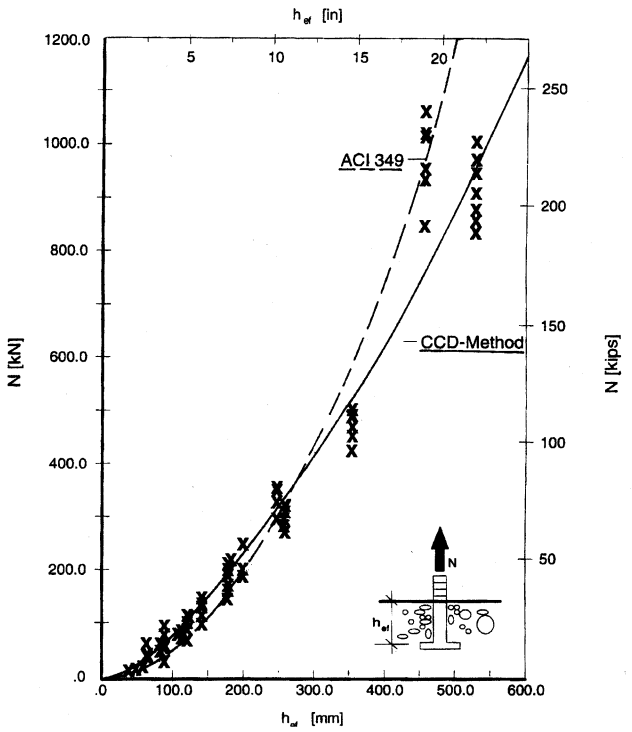

Fig. 21—Concrete breakout load for cast-in situ headed studs, unaffected by edges or spacing effects—Tensile test results and predictions

capacity when tests include many different concrete mixes. The coefficient of variation of expansion anchors is slightly larger, which might be a result of the different load transfer mechanisms.

Note that in Fig. 22 through 24, the average of the ratio $N_{u,test}/N_{u,predicted}$ is higher for the ACI 349 method than for the CCD method. This is due to the fact that the majority of the evaluated data has an effective embedment depth h_{ef} smaller than 150 mm (6 in.). For headed studs with embedments greater than 300 mm (12 in.), ACI 349 predictions become unconservative (Fig. 21). Thus, the average values do not indicate local unconservative cases.

In Fig. 25, results of tests with quadruple fastenings with headed studs are evaluated in the same way as in Fig. 22. The figure indicates that spacing influence is more easily and accurately taken into account by the CCD method than by ACI 349. While the average failure load is predicted correctly by the CCD method, it is significantly overestimated by ACI 349. This can also be seen from Fig. 26, which shows failure loads of groups as a function of the distance s_t between the outermost anchors. Groups with 4 to 36 anchors were installed in very thick concrete specimens loaded concentrically in tension through a rigid load frame to assure an almost equal load distribution to the anchors. Light skin reinforcement was present near the top and bottom surfaces of the specimens and light stirrups were present near the edges in some specimens for handling. The stirrups did not intersect the concrete cone. No reinforcement was present near the fastening heads. These specimens represent the capacity of groups of fasteners installed in plain concrete. Embedment depth and concrete strength were kept constant. In all tests a

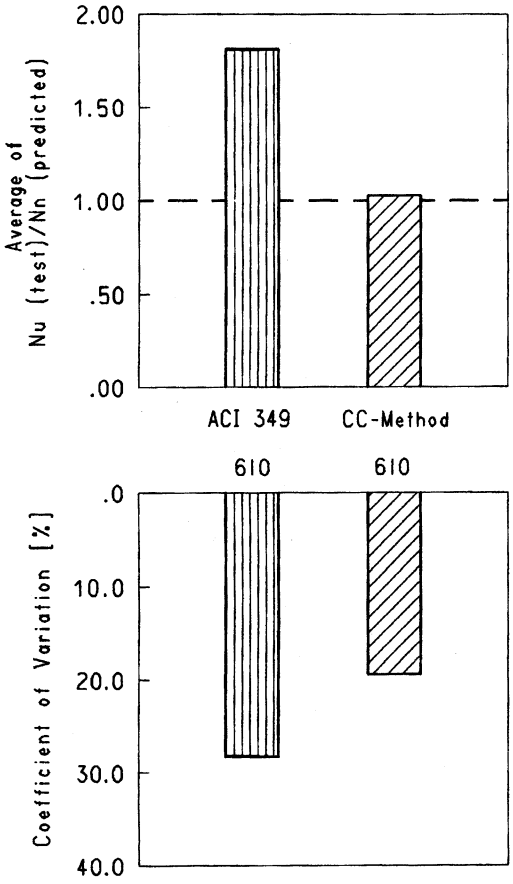

Fig. 22—Comparison of design procedures for post-installed fasteners, unaffected by edges or spacing effects—Tensile loading

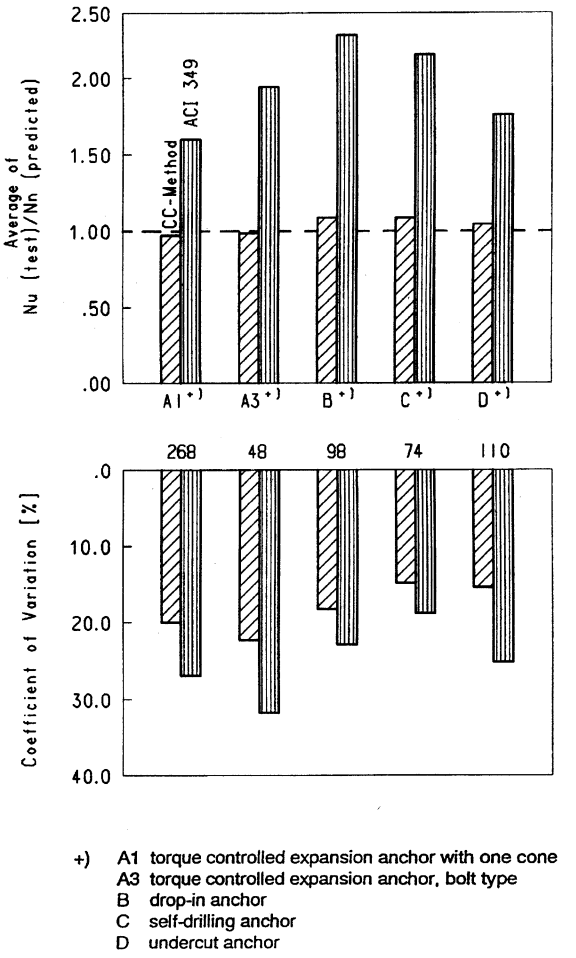

Fig. 23—Comparison of design procedures for post-installed fasteners, unaffected by edges or spacing effects, divided into different fastening systems—Tensile loading

common cone failure was observed. For comparison, single anchors were also tested. For the chosen embedment depth [h_{ef} = 185 mm (7.3 in.)], the capacity of single anchors is predicted almost equally by both methods. However, with increasing spacing of the outermost anchors, the failure load is significantly overestimated by ACI 349 and correctly predicted by the CCD method. This is due to the fact that the critical spacing $s_{cr} = 2h_{ef}$ assumed by ACI 349, which follows from the assumption of a 45-deg cone, is too small. Obviously, provision of special reinforcement designed to engage the failure cones and anchor fastenings back into the block could provide substantial increase in load. This was not investigated in these tests and such increases are not treated in this paper.

In Fig. 27, results of tests with single post-installed fasteners close to the edge are evaluated. The average ratio $N_{u,test}$ to $N_{n,predicted}$ is approximately the same for both methods. However, the coefficient of variation is much smaller for the CCD method and amounts to about the same value as for single fasteners away from edges. This shows that assumptions about the critical edge distance $c_{cr} = 1.5h_{ef}$, and the stress disturbance factor ψ_2, are correct. Note that most of the tests were done with rather shallow anchors (Table 4). For deeper anchors, it would be expected that the CCD method would predict more accurate capacities due to its consideration of size effect and effect of stress disturbance, as well as its assumption of a characteristic edge distance $c_{cr} = 1.5\ h_{ef}$.

Influence of load eccentricity on the failure load of anchor groups is shown in Fig. 28. The eccentricity e_n' is calculated using the general assumptions of the theory of elasticity, i.e., stiff anchor plate, anchor displacement equal to steel elongation, and linear elastic behavior of concrete. It can be seen that the CCD method yields conservative results. This effect is also neglected by ACI 349.

Shear loading

Fig. 29 shows a comparison of results of U.S. and European shear tests performed with single post-installed anchor fastenings in thick concrete members with the design procedure of the CCD method and ACI 349. The tests were performed on concrete with different concrete strengths, different anchor diameters, and different ratios of embedment depth to anchor diameter. Therefore, the measured failure loads were transformed to a concrete strength $f_{cc}' = 25$ N/mm^2 ($f_c' = 3070$ psi), anchor diameter $d_o = 18$ mm (0.71 in.), and a ratio $l/d_o = 8$ by multiplying them with the factor $(25/f_{cc',test})^{0.5} \cdot (18/d_{o,test})^{0.5} \cdot [8/(l/d)]_{test}^{0.2}$. On the average, the concrete breakout loads of the U.S. tests are higher than those of the European tests, especially at smaller edge

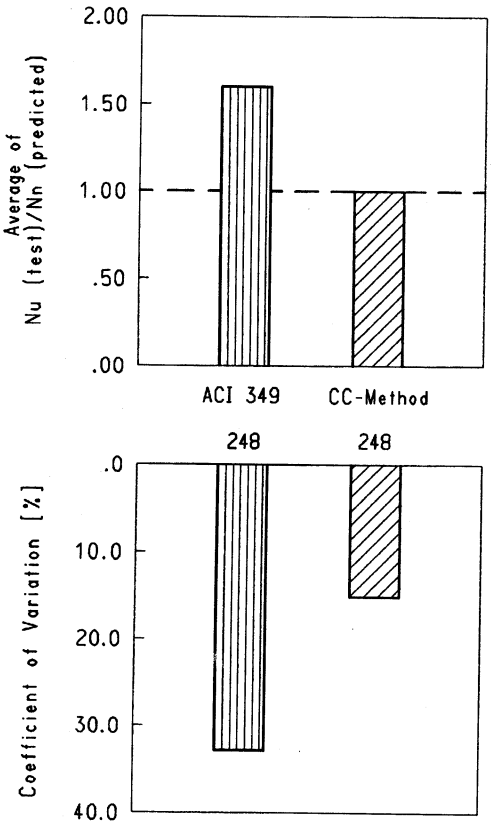

Fig. 24—Comparison of design procedures for cast-in situ headed studes, unaffected by edges or spacing effects—Tensile loading

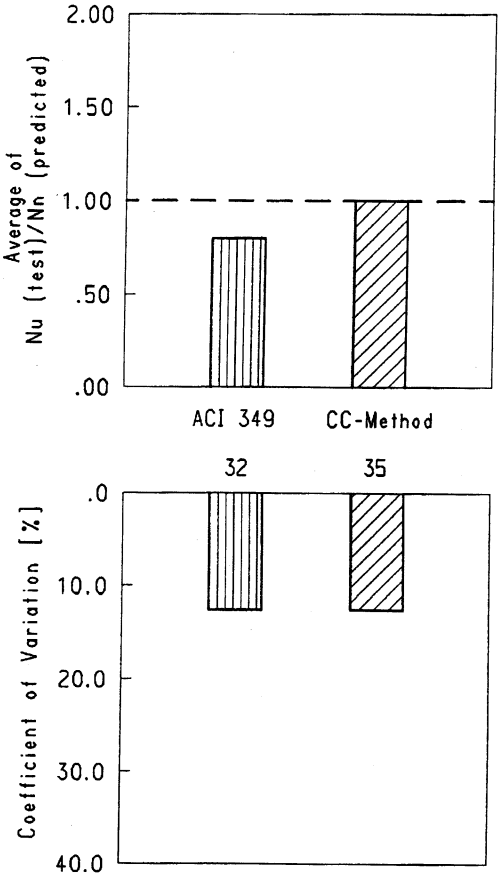

Fig. 25—Comparison of design procedures for quadruple fastenings with cast-in situ headed studes--Tensile loading

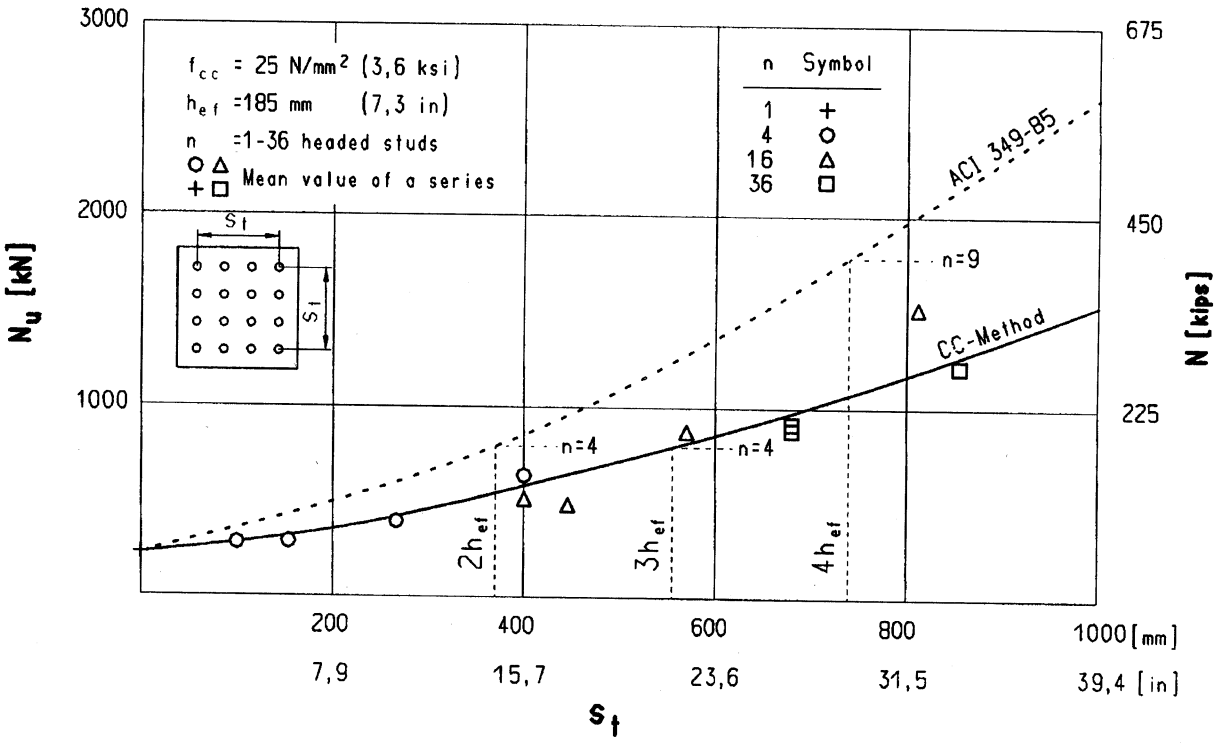

Fig. 26—Actual and predicted loads for groups of cast-in situ headed studs as function of distance between outermost anchors—Tensile loading

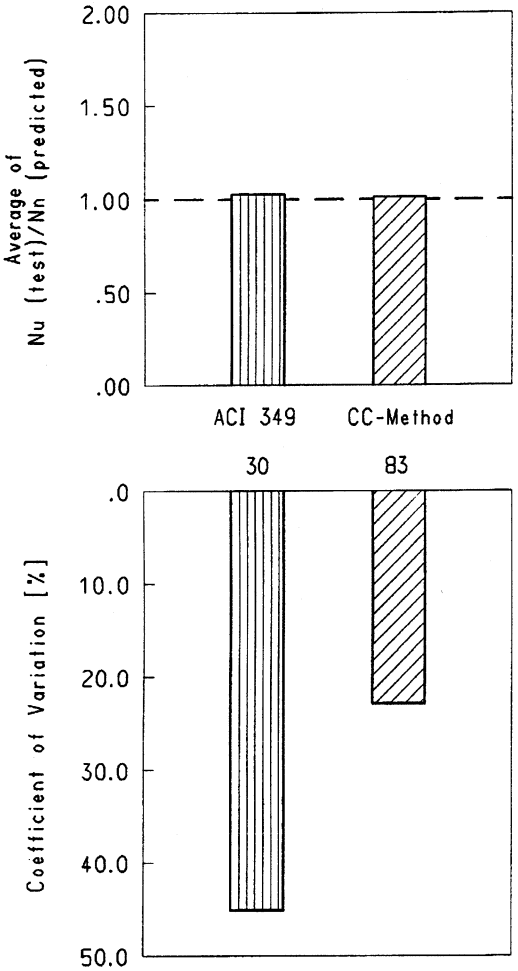

Fig. 27—Comparison of design procedures for single fastenings with post-installed fasteners close to edge—Tensile loading

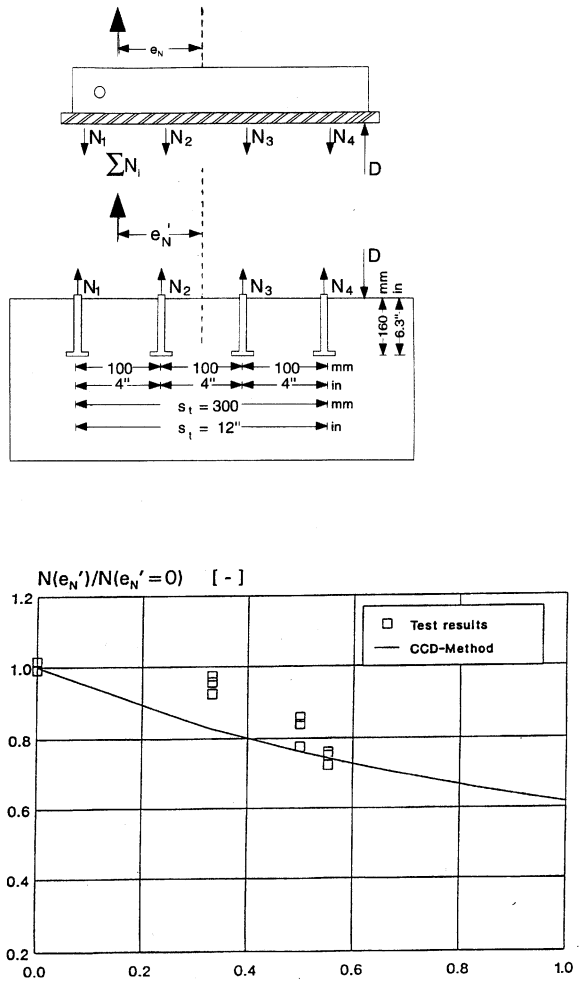

Fig. 28—Comparison of test results on eccentrically loaded line fastenings composed of four cast-in situ headed studs with load predicted by CCD method—Tensile loading[3]

distances. This can be attributed to the absence of a fluoropolymer sheet in the U.S. tests and resulting friction contribution leading to higher shear capacity. The friction contribution relative to the failure load is large for small edge distances.

Failure loads predicted by the CCD method agree well with the average failure loads measured in European tests. On the contrary, ACI 349 is conservative for small edge distances and unconservative for large edge distances. This is, again, probably due to the neglect of size effect by ACI 349. Due to the friction contribution just mentioned, the U.S. test data are predicted more conservatively by both methods.

In Fig. 30 and 31, average values of the ratios $V_{u,test}/V_{n,prediction}$ and corresponding coefficients of variation for post-installed fasteners are given for European and U.S. test data, respectively. The ACI 349 averages are more conservative. This is due to the fact that most tests were done with small edge distances. However, the ACI 349 coefficients of variation are larger. A similar result was found for headed studs.[10]

The results of European tests with double fastenings parallel to the edge and loaded toward the edge (Fig. 32) and tests with single fastenings in thin concrete members (Fig. 33) are similarly evaluated. As can be seen, the CCD method compares more favorably with the test data. For both applications, average failure loads predicted by ACI 349 are unconservative and coefficients of variation are much larger.

CONCLUSIONS

In this study, the concrete capacity of fastenings with cast-in situ headed studs and post-installed anchors in uncracked plain concrete predicted by ACI 349 and the CCD method has been compared with the results of a large number of tests (see Tables 2 through 8). Based on this comparison, the following conclusions can be drawn:

1. The average capacities of single anchors without edge and spacing effects loaded in tension are predicted accurately by the CCD method over a wide range of embedment depths [20 mm (0.8 in.) < $h_{ef} \leq$ 525 mm (20.7 in.)]. For a few post-installed anchors with embedment depths in the 250-mm (10-in.) range, the CCD method was quite conservative. Conversely, ACI 349 underestimates the strength of shallow anchors and is unconservative for quite a number of deep embedments. The same result was found for the predicted capacities of single anchors loaded in shear toward the edge with small or large edge distances, respectively.

This result is due to the fact that ACI 349 assumes the failure load to be proportional to a failure area that increases with the square of the embedment depth. On the other hand, the CCD method takes size effect into account and assumes

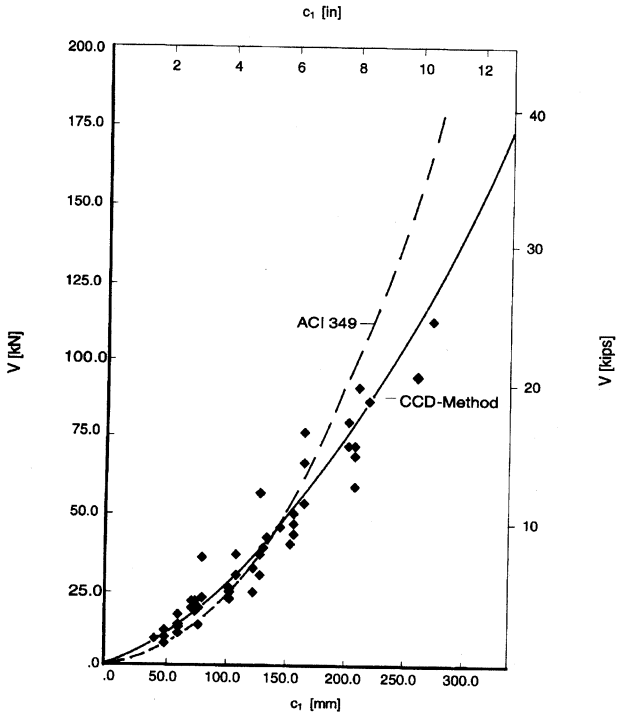

(a)

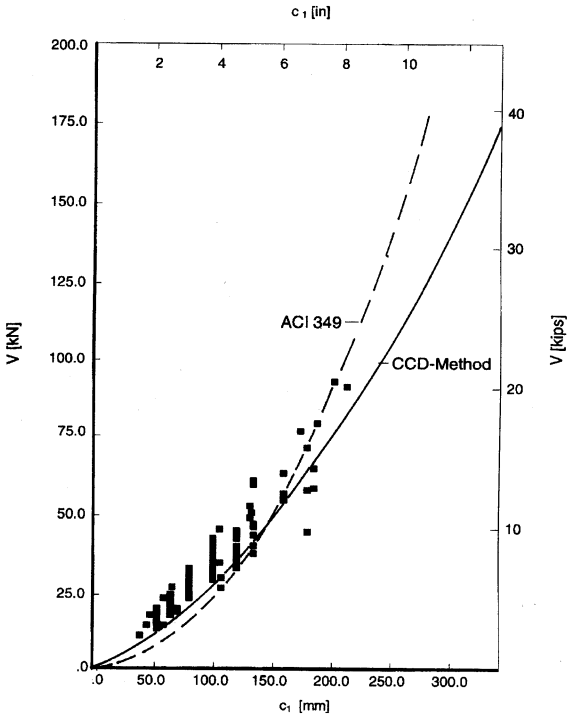

(b)

Fig. 29—Comparison of shear test results with ACI 349 and CCD method for single post-installed fasteners in thick concrete members: (a) European tests; (b) U.S. tests

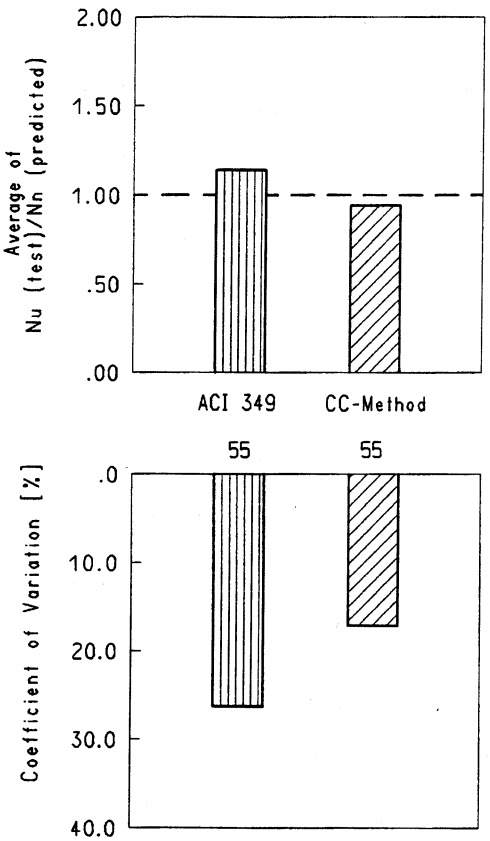

Fig. 30—Comparison of design procedures for European tests with single post-installed fasteners in thick concrete members—Shear loading toward edge

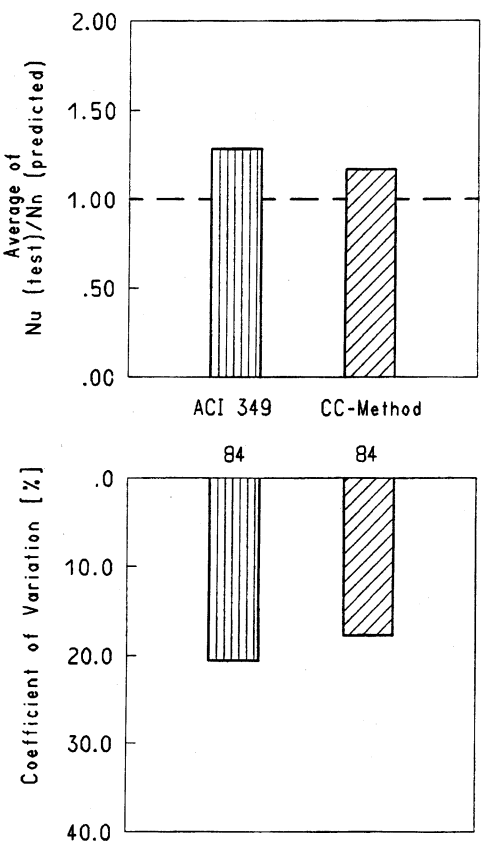

Fig. 31—Comparison of design procedures for U.S. tests with single post-installed fasteners in thick concrete members—Shear loading toward edge

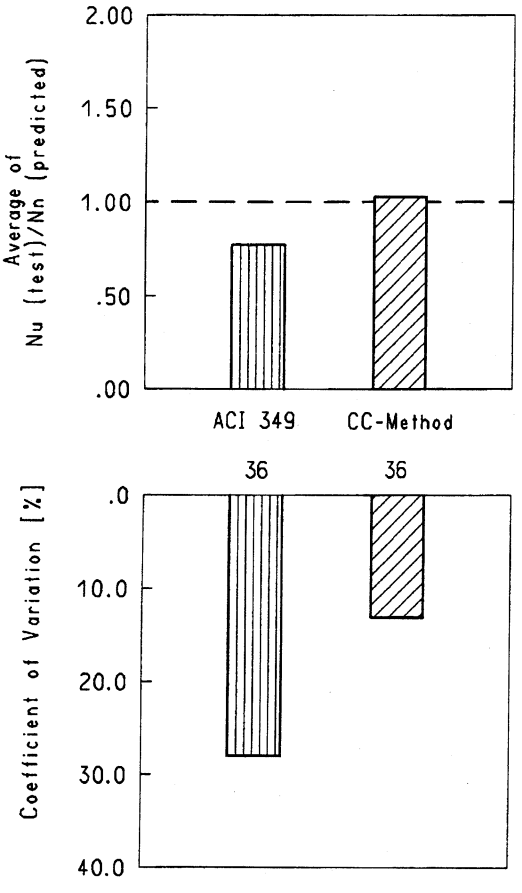

Fig. 32—Comparison of design procedures for double fastenings with post-installed fasteners in thick concrete members (European tests)—Shear loading toward edge

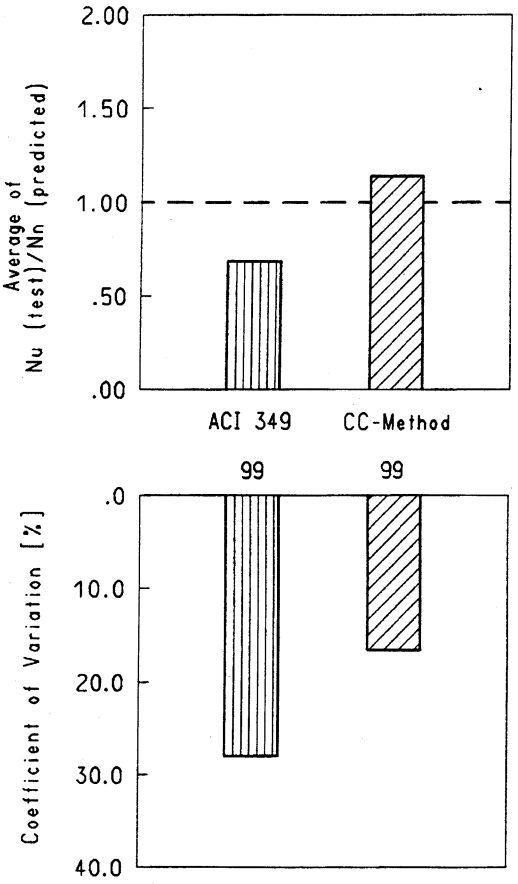

Fig. 33—Comparison of design procedures for European tests with single post-installed fasteners in thin concrete members—Shear loading toward edge

failure load to be proportional to the embedment depth to the 1.5 power.

2. In many applications (for example, anchor groups away from edges loaded in tension, single anchors in thin concrete members loaded in shear, double fastenings in thick concrete members loaded in shear), the capacity is predicted more accurately by the CCD method. Failure loads predicted by ACI 349 for these cases are significantly unconservative. This is mainly due to the fact that ACI 349 assumes a 45-deg failure cone. The CCD method is based on an assumed inclination of the failure surface of about 35 deg, which produces better agreement with test results.

3. In some applications, such as single anchors at the edge loaded in tension, the mean capacity is predicted accurately by both methods. However, the coefficient of variation of the ratio of measured failure load to the value predicted by ACI 349 is rather large ($V \approx 45$ percent).

4. In all applications investigated, concrete capacity is predicted with consistent accuracy by the CCD method. The coefficient of variation of the ratios between measured and predicted capacities is about 15 to 20 percent. This coefficient of variation is equal to or not much larger than the value expected for concrete tensile strength when the test specimens are produced from many different concrete mixes.

5. Calculation of the projected areas is simpler with the rectangular areas of the CCD method, making it user-friendly. In contrast, the circular areas of ACI 349 result in considerable computational complexity.

Summarizing, the CCD method is a relatively simple, transparent, user-friendly, and accurate method for efficient calculation of concrete failure loads for fastenings in uncracked concrete. It is based on a physical model to assist designers in extrapolating the empirical results to other applications. Therefore, this method is recommended for the design of fastenings. It is not incorrect to use the ACI 349 method for many fastening applications. However, since it does not seem universally advantageous and in some applications produces unconservative values, the authors strongly recommend use of the CCD procedures.

CAUTION

It is known that the presence of tensile cracks can substantially reduce the concrete capacity of fasteners.* Some fasteners are not suitable for use in cracked concrete. For those fasteners suitable for use in cracked concrete, it is possible to adjust the uncracked concrete failure loads predicted by the CCD method by using an additional multiplicative factor. This factor results in cracked concrete capacities around 70 percent of uncracked concrete capacities.† Similarly, it is

*,†Eligehausen, R., and Balogh, T., "Behavior of Fasteners Loaded in Tension in Cracked Concrete," accepted for publication in *ACI Structural Journal*.

known that the concrete capacity of fasteners can be enhanced by properly detailed local reinforcement. Such enhancement can be included in design provisions but is outside the scope of this paper.

NOTATION*

c = distance from center of a fastener to edge of concrete

c_1 = distance from center of a fastener to edge of concrete in one direction. Where shear is present, c_1 is in the direction of the shear force

c_2 = distance from center of a fastener to edge of concrete in direction orthogonal to c_1. Where shear is present, c_2 is in the direction perpendicular to shear force

d_o = outside diameter of fastener or shaft diameter of headed stud or headed anchor bolt

d_u = head diameter of headed studs or headed anchors

f_c' = concrete compressive strength, measured on 6 by 12-in. cylinders

f_{cc}' = concrete compressive strength, measured on 200-mm cubes

f_{ct} = concrete tensile strength

h = thickness of concrete member in which a fastener is anchored

h_{ef} = effective embedment depth

n = number of test results

s = distance between fasteners, spacing

s_t = distance between outermost fasteners of a group

V = coefficient of variation

x = ratio of actual to predicted load

x = mean value of x

A_N = projected area, tension

A_V = projected area, shear

CEB = Euro-International Concrete Committee

CS = Czechoslovakia

D = Germany

EUR = Europe

F = France

GB = Great Britain

N = tensile load

S = Sweden

USA = United States of America

V = shear load

α = slope of concrete breakout cone

ϕ = capacity reduction factor for safety considerations

REFERENCES

1. ASTM ZXXX, "Standard Specification for Performance of Anchors in Cracked and Non-Cracked Concrete Elements," Draft 1, Mar. 22, 1993.

2. Furche, J., and Eligehausen, R., "Lateral Blowout Failure of Headed Studs near a Free Edge," *Anchors in Concrete—Design and Behavior*, SP-130, American Concrete Institute, Detroit, 1991, pp. 235-252.

3. Zhao, G., "Befestigungen mit Kopfbolzen im ungerissenen Beton (Fastenings with Headed Studs in Uncracked Concrete)," PhD thesis, University of Stuttgart, 1993.

4. ACI Committee 349, "Code Requirements for Nuclear Safety Related Concrete Structures (ACI 349-85)," American Concrete Institute, Detroit, 1985.

5. *PCI Design Handbook,* 4th Edition, Precast/Prestressed Concrete Institute, Chicago, 1992.

6. Eligehausen, R.; Fuchs, W.; and Mayer, B., "Loadbearing Behaviour of Anchor Fastenings in Tension," *Betonwerk & Fertigteil-Technik* (Wiesbaden), No. 12, 1987, pp. 826-832; and No. 1, 1988, pp. 29-35.

7. Eligehausen, R., and Fuchs, W., "Loadbearing Behaviour of Anchor Fastenings under Shear, Combined Tension and Shear or Flexural Loading," *Betonwerk & Fertigteil-Technik* (Wiesbaden), No. 2, 1988, pp. 48-56.

8. Rehm, G.; Eligehausen, R.; and Mallée, R., "Befestigungstechnik (Fastening Technique)," *Betonkalender 1992,* V. II, Ernst & Sohn, Berlin, 1992, pp. 597-715. (in German)

9. Eligehausen, R., "Vergleich des κ-Verfahrens mit der CC-Methode (Comparison of the κ-Method with the CC-Method)," *Report* No. 12/16-92/7, Institut für Werkstoffe im Bauwesen, Universität Stuttgart, 1992. (in German)

10. Fuchs, W., "Entwicklung eines Vorschlags für die Bemessung von Befestigungen (Development of a Proposal for the Design of Fastenings to Concrete)," Report to the Deutsche Forschungsgemeinschaft, Feb. 1991. (in German)

11. Klingner, R. E., and Mendonca, J. A., "Tensile Capacity of Short Anchor Bolts and Welded Studs: A Literature Review," ACI JOURNAL, *Proceedings* V. 79, No. 4, July-Aug. 1982, pp. 270-279.

12. Klingner, R. E., and Mendonca, J. A., "Shear Capacity of Short Anchor Bolts and Welded Studs: A Literature Review," ACI JOURNAL, *Proceedings* V. 79, No. 5, Sept.-Oct. 1982, pp. 339-349.

13. ACI Committee 318, Letter Ballot LB 93-5, CB-30, Proposed Chapter 22, Fastening to Concrete, 1993.

14. ACI Committee 349, "Code Requirements for Nuclear Safety Related Concrete Structures (ACI 349-76)," American Concrete Institute, Detroit, 1976.

15. ACI Committee 349, "Design Guide to ACI 349-85," American Concrete Institute, Detroit, 1988.

16. Cook, R. A., and Klingner, R. E., "Behavior and Design of Ductile Multiple-Anchor-To-Steel-Connections," *Research Report* No. 1126-3, Center for Transportation Research, University of Texas at Austin, 1989.

17. Bazant, Z. P., "Size Effect in Blunt Fracture, Concrete, Rock, Metal," *Journal of Engineering Mechanics,* ASCE, V. 110 No. 4, 1984, pp. 518-535.

18. Bode, H., and Roik, K., "Headed Studs—Embedded in Concrete and Loaded in Tension," *Anchorage to Concrete,* SP-103, G. B. Hasselwander, ed., American Concrete Institute, Detroit, 1987, pp. 61-88.

19. Eligehausen, R., and Sawade, G., "Fracture Mechanics Based Description of the Pull-Out Behaviour of Headed Studs Embedded in Concrete," *Fracture Mechanics of Concrete Structures. From Theory to Applications,* L. Elfgren, ed., Chapman & Hall, London, 1989, pp. 263-281.

20. Eligehausen, R., and Ozbolt, J., "Size Effect in Anchorage Behaviour," *Proceedings, European Conference on Fracture Mechanics, Fracture Behaviour and Design of Materials and Structures,* Turin, Oct. 1991, pp. 17-44.

21. Eligehausen, R.; Bouska, P.; Cervenka, V.; and Pukl, R., "Size Effect on the Concrete Failure Load of Anchor Bolts," *Fracture Mechanics of Concrete Structures,* Elsevier Applied Science, 1992, pp. 517-525.

22. Eligehausen, R., and Balogh, T., 'CC-Method (Concrete Capacity Method)," *Report* No. 12/15-92/1, Institut für Werkstoffe im Bauwesen, Universität Stuttgart, 1992.

23. Eligehausen, R.; Fuchs, W.; Lotze, D.; and Reuter, M., "Befestigungen in der Betonzugzone (Fastenings in the Concrete Tensile Zone)," *Beton und Stahlbetonbau* (Berlin), No. 1, 1989, pp. 27-32; and No. 2, pp. 71-74. (in German)

24. Riemann, H., " 'Extended κ-Method' for the Design of Fixing Devices as Exemplified by Headed Stud Anchorages," *Betonwerk & Fertigteil-Technik* (Wiesbaden), No. 12, 1985, pp. 808-815.

25. Paschen, H., and Schönhoff, T., "Untersuchungen über in Beton eingelassene Scherbolzen aus Beton (Investigations about Shear Bolts Made from Reinforcing Bars in Concrete)," *Deutscher Ausschuss für Stahlbeton* (Berlin), No. 346, 1983.

26. Fuchs, W., "Tragverhalten von Befestigungen unter Querlast im ungerissenen Beton (Behaviour of Fastenings under Shear Load in Uncracked Concrete)," Mitteilungen No. 1990/2, Institut für Werkstoffe im Bauwesen, Universität Stuttgart, 1990.

27. Stichting Bouwresearch, "Uit beton stekende ankers (Anchors Sticking Out of Concrete)," Report of the Study Commission B7, V. 27, 1971.

28. Maxi-Bolt Load Test Program, Arkansas Nuclear One, *Engineering Report* 92-R-0001-01.

29. Burdette, E. G.; Perry, T. C.; and Funk, R. R., "Load Relaxation Tests of Anchors in Concrete," *Anchorage in Concrete,* SP-103, G. B. Hasselwander, ed., American Concrete Institute, Detroit, 1982, pp. 133-152.

*Notations for specific design procedures are defined in sections related to that procedure.